Excited electron orbit collapse and atomic spectra

1981 Sov. Phys. Usp. 24 775

(http://iopscience.iop.org/0038-5670/24/9/R03)

Excited electron orbit collapse and atomic spectra

R. I. Karaziya

Institute of Physics, Academy of Sciences of the Lithuanian SSR
Usp. Fiz. Nauk **135**, 79–115 (September 1981)

The reasons for the two-well potential in free atoms and the collapse of the orbit (or wave function) of an electron are discussed. Theoretical data on the dependence of the collapse on the atomic number, the degree of ionization, the configuration, the many-electron quantum numbers, etc., are put in systematic form. A similar effect occurs for a free electron moving in an atomic field. Various manifestations of the collapse and the potential barrier in the energy spectra are discussed: an anomalous behavior of the quantum defect, a nonmonotonic variation in the type of binding in an isoelectronic series, a broadening of the energy spectrum, and a pronounced mixing of configurations. Effects of the collapse and the barrier in photoabsorption spectra are also discussed: a suppression of the Rydberg series, a shift of the absorption edge, the appearance of giant absorption resonances corresponding to transitions in the discrete spectrum, and the alignment of ions during photoionization of atoms. Experimental data which furnish evidence that the interaction of slow electrons with atoms is quasiresonant in the case of a two-well potential are reviewed briefly.

PACS numbers: 31.20.Tz, 32.70.Jz, 32.80.Fb

CONTENTS

1. INTRODUCTION

The introduction of new methods in optical spectroscopy and the development of vacuum-UV and x-ray spectroscopy have stimulated more extensive research on the properties of atoms, especially their excited states. It has been found that the traditional picture of Rydberg series and of monotonic variation in the characteristics of atoms in an isoelectronic series or in the series of neutral atoms during the filling of a shell is sometimes disrupted. The primary cause of these anomalous features in atomic properties is the so-called collapse of the quantum orbit (or wave function) of an excited electron, or simply "electron collapse."

This effect was predicted by Fermi[1] way back in 1928. Working from the solutions of the statistical Thomas–Fermi equation, he showed that the radius of the 4f orbit decreases sharply as the atomic number increases from 55 to 60. The orbit converts from an outer orbit into an inner orbit; the conversion is responsible for the formation of the rare earth elements. The changes in the nature of the wave functions of the 4f and 5f electrons at the beginning of the lanthanide and actinide groups were studied in more detail, on the basis of the same model, by Fermi's student Maria Goep-

 0038-5670/81/090775-20$01.10

pert-Mayer. She showed that the reason for the phenomenon lay in the particular shape of the effective potential in which the excited f electron is moving; a potential with two wells separated by a positive potential barrier. The deepening of the inner well with increasing nuclear charge eventually leads to an abrupt decrease in the radius of the quantum orbit, i.e., to a collapse of this orbit (the term "collapse" was not used in these early papers and was introduced later by Cowan[3]).

Electron collapse attracted little interest through the 1960's, and the greater interest it has begun to win since then is due entirely to the intense study of the properties of excited atomic states.

It has been shown that the collapse occurs not only for f electrons but also for excited d electrons.[3,4] The collapse can occur not only in a series of neutral atoms but also in an isoelectronic series,[3] upon a change in electron configuration,[5] or even upon a change in the many-electron state of an atom.[6,7] The collapse leads to important changes—by factors ranging from several units to several orders of magnitude—in various one-electron and many-electron characteristics of atoms which depend on the wave function of an excited electron: the average distance from the electron to the nucleus, the binding energy, the electrostatic and spin–orbit interactions between shells, oscillator strengths, etc.[3,8] These changes can be seen in the energy spectra of the atoms and in the photoabsorption spectra as several anomalous features and nonmonotonic variation from one element to another.

If a free electron is moving in the field of an atom whose effective potential contains an inner well bounded by a positive potential barrier, then at the electron energy equal to the energy of a quasistationary level in the well there is an abrupt penetration of the radial wave function of the free electron into the atom.[9-11] This phenomenon, which is somewhat analogous to the collapse of an electron of a discrete spectrum,[12,13] causes shape resonances in the photoionization spectra[12] and in the scattering of electrons by atoms,[9,14] suppression of the Auger electron emission,[15] and the appearance of a sharp peak in the bremsstrahlung spectrum,[16,17] among other effects.

Similar effects have been observed in the absorption spectra of molecules and solids, but there the reasons for the formation of the potential barrier are more complicated and have received less study. The results available in those cases have been put in systematic form by Fano[18] and Dehmer.[19]

In the present review we will discuss the effects of the collapse and of the potential barrier in free atoms. These questions have been the subject of only a single previous review, of non-Rydberg effects in absorption spectra.[12] The lack of a really satisfactory systematic classification of data on collapse in atoms is one of the reasons why this effect has received comparatively little study and is sometimes neglected in research on atomic spectra. Although collapse occurs only for certain elements, for which the configuration contains an excited electron with $l \geq 2$, or for a comparatively narrow interval of energies near the threshold, it can have important effects in these cases, changing various properties of the atoms. Collapse therefore deserves the attention of both experimentalists and theoreticians.

In the following section we will give a general picture of the reasons for the formation of a two-well effective potential and for the collapse of an electron orbit. In Sec. 3 we will use the solutions of the Hartree–Fock equations to analyze the particular features of the orbital collapse of various electrons and the effect of the collapse on the one-electron and many-electron properties. The subsequent sections will deal with manifestations of collapse and of the potential barrier in atomic energy spectra, in photoabsorption spectra, and in the interaction of low-energy electrons with atoms.

2. THE TWO-WELL EFFECTIVE POTENTIAL AND COLLAPSE

a) Conditions for the formation of a two-well potential

Collapse has been studied primarily in the nonrelativistic one-electron approximation with separable variables. The one-electron model is very graphic, and it yields a qualitative, and frequently quantitative, explanation for the basic aspects of collapse.

Let us assume that the wave function of an atom is the antisymmetrized product of one-electron wave functions with coupled spins and that a separation into angular, spin, and radial parts can be carried out in the one-electron wave functions. The angular one-electron wave functions are the standard spherical harmonics, and only the radial wave functions depend on the properties of the particular atom. The behavior of these radial wave functions is determined by the effective potential[1)]

$$\Phi(nl|r) = V(nl|r) + \frac{l(l+1)}{2r^2}, \tag{2.1}$$

where $V(nl|r)$ is the potential of the electrostatic field produced by the nucleus and the outer electrons, and the second term in (2.1), which arises upon separation of variables in the one-electron Schrödinger equation, corresponds to the classical centrifugal energy.

The potential is conveniently written as

$$V(nl|r) = -\frac{Z(nl|r)}{r}, \tag{2.2}$$

where $Z(nl|r)$ is the effective nuclear charge, which generally depends on the distance from the nucleus.

In the hydrogen-like approximation, $Z(nl|r)$ is a constant:

$$Z^H(nl\,|\,r) = Z - \sigma(nl), \tag{2.3}$$

where Z is the nuclear charge and $\sigma(nl)$ is the screen-

1)Here and below, except where otherwise stipulated, the system of atomic units is being used.

ing constant. In this approximation, $\Phi(nl|r)$ always has a single well.

If the effective potential is to have a more complicated shape, with several wells, the effective charge must depend on r: In a certain radial interval this charge must vary as r^{-n} ($n \geq 1$), and in this case the two terms in (2.1) can compete with each other.[20]

This condition is already met in the case of the Thomas–Fermi potential.[21] In the interval $\mu < r < 4\mu$ ($\mu \approx 0.94Z^{-1/3}$) the Thomas–Fermi function $r\varphi(r)/\mu$ has a broad maximum, and the effective charge in this integral can be approximated by[20]

$$Z^{\mathrm{TF}}(nl|r) \approx \frac{0.9Z\mu}{r}. \qquad (2.4)$$

The formation of the two-well potential depends on the magnitude of the centrifugal term, which increases quadratically with increasing l. The effective Thomas–Fermi potential contains a positive barrier for electrons with $l \geq 3$, and if the asymptotic form of this potential is corrected by $-2/r$ then it also contains a potential barrier for d electrons.[4,22]

This condition is also satisfied by the (more accurate) Hartree–Fock potential. If there is only a single electron in the nl excited shell, the effective Hartree–Fock charge found from the Hartree–Fock equations for the average energy (HF-av) is given by[23]

$$Z^{\mathrm{HF}}(nl|r) = Z - \sum_{\substack{n'l' \\ (n'l' \neq nl)}} N_{n'l'} Y_0(n'l', n'l'|r) + Z^{\mathrm{ex}}(nl|r). \qquad (2.5)$$

Here $N_{n'l'}$ is the number of electrons in the $n'l'$ shell, and the integral function $Y_0(n'l', n'l'|r)$ describes the screening effect of the $n'l'$ electron on the nl electron[23]:

$$Y_0(nl, nl|r) = \int_0^r P^2(nl|r_1)\,dr_1 + r\int_r^\infty r_1^{-1}P^2(nl|r_1)\,dr_1. \qquad (2.6)$$

Here $P(nl|r)$ is the radial one-electron wave function, and $Y_0(nl, nl|r)$ is a positive function which increases monotonically from 0 to 1 as r increases.[23] In practice, this function reaches a unit asymptotic value at a distance from the nucleus equal to several times the distance from the nucleus to the main peak in the wave function.

The term $Z^{\mathrm{ex}}(nl|r)$ stems from the exchange part of the Hartree–Fock equation. The nonlocal exchange potential is frequently approximated by the local statistical Slater potential[23,24] (the Hartree–Slater potential; a modification of it is the Herman–Skillman potential,[25] which incorporates self-effects and gives the function the correct asymptotic behavior. In those cases in which a local potential is used in solving the Hartree–Fock equations, it can be written in a local form for a more graphic representation of the effective potential by dividing the exchange term in the Hartree–Fock equation by the solution of the equation [in cases in which $P(nl|r)$ has nodes, the potential is smoothed over these points[26]]. The function $Z^{\mathrm{ex}}(nl|r)$ obtained in this manner agrees well with its statistical approximation.[27]

The effective potential according to the Hartree–Fock equations for the average energy is determined primarily by the first two terms in (2.5). For configurations with an excited core this approximation is sometimes inadequate, and, if so, the Hartree–Fock equations should be solved for each term[23,24] (HF-t). In this case, additional (algebraic) terms which depend on the partricular (energy) term appear in the direct and exchange parts of the potential and of the effective charge. As we will show in the following section, the term-dependent exchange part of the charge may also be important in the formation of the potential barrier.

In the case of an electron with an orbital angular momentum $l \geq 2$ a competition may arise among the Coulomb attraction of the nucleus, the screening effect of the other electrons, and the centrifugal repulsion in a certain radial interval, with the result that a two-well potential forms (Fig. 1).

At small values of r the effective charge approaches a constant value $Z(nl)$, and the behavior of $\Phi(nl|r)$ is determined by the centrifugal term, which prevents electrons with $l \neq 0$ from entering the nuclear volume. With increasing distance from the nucleus the Coulomb attraction becomes comparable to the centrifugal repulsion, and a potential well forms. Because of the increase in the screening of the nucleus by the inner electrons, however, $Z(nl|r)$ falls off rapidly with increasing r, and at 1–3 a.u. the centrifugal term may again become predominant; a potential barrier arises and assumes small positive values.[22] At large values of r effective potential is determined by the Coulomb potential with $Z(nl|r) \approx 1$; an external potential well of a hydrogen-like nature forms. Because of the slow decay of the Coulomb potential, this well is wide but shallow.

b) Energy levels and wave function in the case of a two-well potential

Only $Z^{\mathrm{ex}}(nl|r)$ depends on $P(nl|r)$ in (2.5), so that the potential for the excited electron depends only weakly on the quantum number n, and $\Phi(nl|r)$ can be approximated as being the same for all series of excited states with the same value of l but different values of n. [This assumption becomes better as n increases; at small values of n, the differences in $\Phi(nl|r)$ can sometimes be important,[28,29] especially if some of the wave functions are collapsed, while other are uncollapsed.]

If the barrier were infinitely high the two wells would have independent systems of energy levels. For a low barrier there is a common system of levels, which

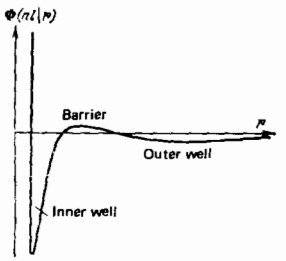

FIG. 1. Two well effective potential (schematic drawing).

are distributed between the two wells.[2,30] Since the inner well is narrow, it contains only a few levels, perhaps none at all for certain values of Z. In this case the principal maxima of all the wave functions of the nl electrons (with a given value of l) in the corresponding configurations with this excited electron are localized in the outer well, far from the nucleus.

As the nuclear charge increases, the inner well becomes deeper and broader. When this well acquires an energy level below the ground level in the outer well, there is a sudden displacement of the wave function of the first excited electron of the given series to the inner well. Consequently, an electron with $n=l+2$ in the corresponding configuration occupies a lower level in the outer well; since this well is hydrogenlike, one node of the radial wave function of the electron is shifted to the inner well or to the barrier and becomes similar to the uncollapsed function $P(nl|r)(n=l+1)$ (Refs. 30 and 31). [If, in the calculation of $P(nl|r)(n=l+2)$, this wave function is not made orthogonal with respect to the collapsed wave function $P(nl|r)(n=l+1)$, as is necessary when a variational method is applied to an excited state, then even a node-free wave function may emerge as if it were a second solution for $P(nl|r)(n=l+1)$ (Refs. 32 and 33).] During the collapse of the wave function of the first state, any other wave function in the given series $P(nl|r)$ becomes similar to the uncollapsed wave function $P(n-1l/r)$ near the outer well, and the quantum defect of the series changes by one.[30]

Figure 2 illustrates the formation of the inner well and the change of the effective barrier in the series of neutral atoms. Since the centrifugal term depends strongly on the orbital angular momentum of the electron, the barrier is considerably higher for f electrons than for d electrons. The barrier height varies in a nonmonotonic manner through the series of elements; in the Herman–Skillman approximation the height is greatest for Cu, Ag (or Pd), and Au, after the 3d, 4d, and 5d shells, respectively, are filled.[22] After these elements, a shell with a value of n greater by one begins to be filled, and the contribution of the new electron to the effective charge $Y_0(nl,nl|r)$ near the barrier is less effective in cancelling the unit increase in the charge, so that the barrier is lowered.

c) Electron collapse in ions and atoms

The removal of an $n'l'$ electron from an atom corresponds to elimination of the corresponding term $Y_0(n'l',n'l'|r)$ from (2.5). Although the relaxation of the wave functions of the other electrons partially cancels this increase in the effective charge, it still increases over the entire range of distances during ionization, especially in the asymptotic region (Fig. 3). As the degree of ionization is raised, the curves of $Z(nl|r)$ and $l(l+1)/2r$ intersect at only a single point. The effective potential barrier in the isoelectronic series thus lowers rapidly, becomes negative, and disappears (Fig. 4). The lowering of the barrier upon ionization of the atom becomes more pronounced with decreasing average distance from the nucleus to the electron which is removed [or as $Y_0(nl,nl|r)$ near the barrier approaches its asymptotic value]. Consequently, the electron collapse resulting from the existence of a potential barrier can occur only in neutral atoms, negative ions, and positive ions of low charge.

It has been suggested[30] that the displacement of the primary maximum of the wave function from the outer well to the inner well should always occur abruptly, i.e., that within the framework of the self-consistent method it would not be possible to find a wave function which had a substantial amplitude in both wells. As it turns out, this view is correct only in the case of a single excited electron with a large value of l in neutral atoms, where there is a high postive potential barrier. The characteristic example of this clearly defined collapse is the change in the wave function of the 4f electron between Ba and La (Fig. 5).

If the potential barrier is only poorly defined, e.g., for an excited d electron or for an ion, the electron collapse may occur gradually, over several atoms,[34] or (for a given atom) upon an increase in the ionization

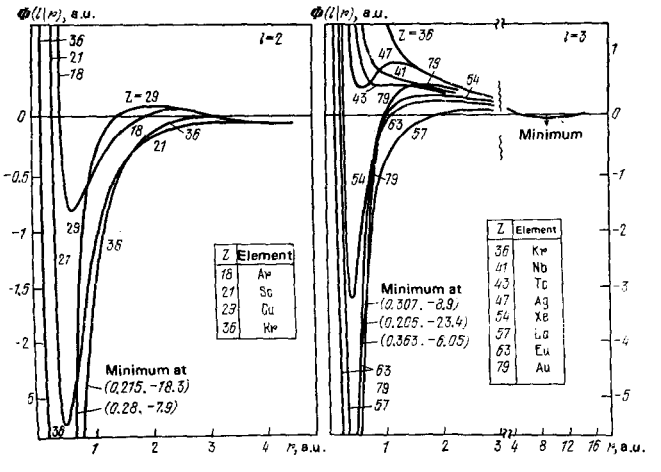

FIG. 2. Change in the effective potential for d and f electrons as a function of the atomic number[20] (the Herman–Skillman potential).

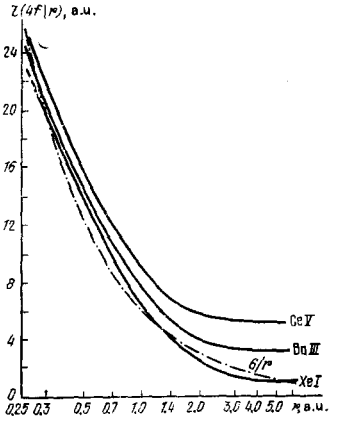

FIG. 3 The effective charge $Z(4f|r)$ for various degrees of ionization in the isoelectronic series $Xe\,I\,4d^9 4f$ and the function[27] $l(l+1)/2r$ (the Hartree-Fock potential for the average energy).

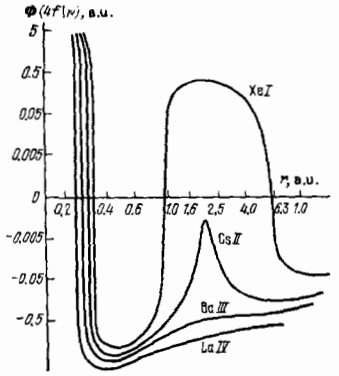

FIG. 4. Change in the effective potential $\Phi(4f|r)$ in the isoelectronic series Xe I $4d^9 4f$ (the Hartree-Fock potential for the average energy).

potential (Fig. 6) or a change in configuration.[5] In these cases, a hybrid wave function may arise which is distributed in both wells and whose principal maximum has two humps (Fig. 7). In this case, for Ba II, because of differences in the effective potential $\Phi(nl|r)$ (because of its dependence on the radial wave function of the nl excited electron), the wave function $P(5f|r)$ is "pulled" into the inner well more than $P(4f|r)$. A two-humped wave function for a 4f electron has also been found for Cs I $4d^9 4f^2$, in which case the excited shell has several electrons.[35]

Even in cases without a potential barrier (for an electron with $l \geq 2$ in the field of an atom which is ionized relatively strongly or for a p electron) near the atomic number at which the given electron appears in the basic configuration, there may be a comparatively rapid change in the localization of the electron.[36,37] This effect can be seen, for example, in the anomalous change in oscillation strengths and in the positions of the energy levels in the isoelectronic series as a function of Z (Ref. 38). In this case the contraction of the wave function results from a change in the shape of the well and from a lowering of an energy level in an asymmetric well. It would hardly be possible to draw

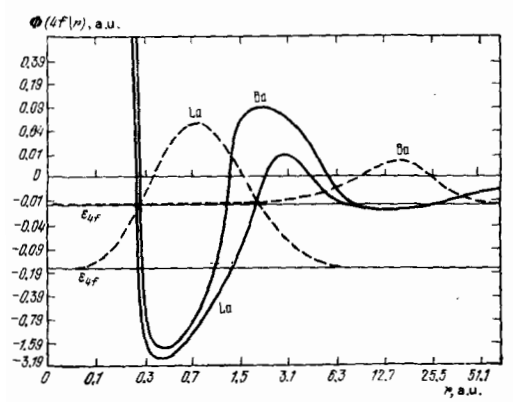

FIG. 5. Collapse of a 4f electron between BaI6s4f and LaI6s5d4f (Ref. 30). Solid curves—The potential $\Phi(4f|r)$ (the Hartree–Slater potential); dashed curves—the radial wave function $P(4f|r)$ (this function is drawn in linear scale; the origin on this scale corresponds to the one-electron energy).

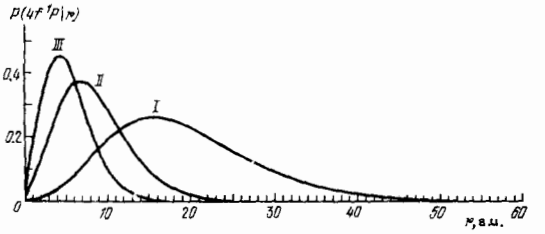

FIG. 6. Gradual contraction of the radial wave function of the 4f electron for Ba$4d^9 4f^1$P upon an increase in the degree of ionization.[8] The wave function is the solution of the Hartree-Fock equations for each term. The curves are labelled with the degree of ionization.

a definite boundary between gradual collapse in the case of a poorly defined negative barrier, on the one hand, and this contraction of the wave function, on the other, so that if we take the term "electron collapse" in a broader sense, as a rapid change in the electron wave function, then this case would also be covered.

d) Calculation errors in the case of a collapsing electron. Many-electron effects

In the case of critical equilibrium with a two-well potential, even a slight change in the potential can lead to a pronounced change in the localizations of the electron. Such a situation arises if the value of Z for the given atom is approximately equal to the critical charge Z_c (generally not an integer), at which there should be a sudden displacement of the principal maximum of the wave function from the outer well to the inner well. Near Z_c, serious difficulties arise in attempts to solve the Hartree–Fock equations, and failure to observe rigorously all the conditions on the wave function may lead to nonphysical solutions. In such cases it will not always be possible to obtain qualitative agreement with experiment, even if certain many-electron effects are taken into account (see Subsection 4 c).

As the electron collapse becomes more abrupt, the results calculated near Z_c become more sensitive to the particular approximation used, but the range of Z over which the results depend strongly on the approximation becomes narrower. For an uncollapsed electron, correlation effects are comparatively slight—because the wave function of this electron overlaps only slightly with those of the core electrons. In excited configurations with two unfilled shells a more impor-

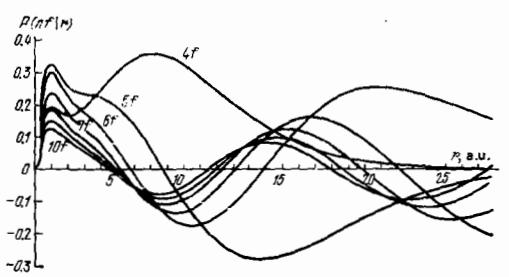

FIG. 7. Radial wave functions of the excited nf electron for Ba II, distributed in both potential wells[29] (solutions of the Hartree–Fock equations for the average energy).

tant role may be played by the electrostatic interaction, which depends on the term and which is usually averaged over the terms in the course of solving the Hartree–Fock equations. In such cases, the Hartree–Fock equations for each term must be solved.

Comparison of the results calculated in the approximation of the Hartree–Fock equations for each term with experimental data (Secs. 4 and 5) shows that this approximation yields results which are qualitatively correct, and in many cases quantitatively correct, even at $|Z - Z_c| > 1/2$ for elements of intermediate weight and even for the lathanides. [Even for wave functions distributed in both wells (Fig. 7) the Hartree–Fock results correspond to the experimental data and explain the anomalous features in the behavior of the quantum defect and oscillator strengths.[29]] Only if Z_c is very nearly equal to an integer can large errors occur. In such cases, great caution must be observed in deriving and interpreting theoretical results. Comparison with experimental data usually yields a definite answer, since electron collapse leads to pronounced and characteristic changes in the atomic spectra. On the other hand, the sensitivity of the wave function to the particular approximation used near Z_c can be exploited to evaluate the accuracy of the wave function.

A graphic representation of the potential barrier and of the collapse of a one-electron wave function can be found not only in the one-electron approximation but also when certain many-electron effects are taken into account. For example, in the expanded calculation method which incorporates the radial correlation, each electron in a shell of equivalent electrons is described by a separate radial wave function; for a certain atom, one of those wave functions may be collapsed while the others are still localized in the outer wall. The concept of a one-electron effective potential also remains valid in the multiconfigurational approximation, but in this case additional configurational terms appear in the effective potential.[24]

The one-electron approximation and the effective potential are not used explicitly in some correlation methods, e.g., the method of incomplete separation of variables,[40] and the same is true in those approximations in which the wave functions of the initial and final states of an atom are refined simultaneously. The random-phase approximation with exchange (RPAE) is a method of the latter type which is widely used in work on the interaction of atoms with electromagnetic radiation.[20,41,42] Below, we will look at some of the results found by the RPAE method for the photoabsorption cross sections, in which effects of the electron collapse and the potential barrier can be seen (although the collapse itself was not studied in those papers). We cannot go into detail on the ideas behind this method (these ideas are set forth quite thoroughly in Refs. 41–43, for example), but we can summarize it by saying simply that it uses perturbation-theory methods to treat the dynamic polarizability of an atom subjected to an external agent. Only certain types of diagrams, which are important in the case of a dense electron gas, are taken into account.

3. PARTICULAR FEATURES OF THE COLLAPSE OF DIFFERENT ELECTRONS

Before taking up the effect of electron collapse on various atomic spectra, we will put in systematic form the theoretical results on the dependence of the effect on the atomic number, the configuration, the many-electron state, etc.

a) Configurations corresponding to excitation from an outer shell

Table I shows which elements exhibit collapse of various electrons if the core has a normal configuration, i.e., if only one valence electron is excited. The statistical method overestimates the values of Z at which the abrupt change in the one-electron wave function occurs. The nonrelativistic Hartree–Fock method and the relativistic Dirac–Fock method lead to values in good agreement with experimental data found from optical spectra.[45] Significantly, the results calculated by the nonrelativistic and relativistic methods differ only slightly even at quite large values of Z.

According to Table I, collapse of an electron occurs for an element which in the periodic table precedes an element containing the given electron in a normal atomic configuration. The increase in the binding energy upon collapse is not sufficient for the appearance of this electron in the normal configuration, but already for the following element the level in the narrow inner well has dropped below the levels of other free one-electron states.

The size of the centrifugal term in (2.1) and the barrier height depend strongly on the orbital angular momentum of the electron; thus the g and f electrons have the most clearly defined two-well potentials.[30] The angular momentum l also affects the position and magnitude of the minimum of the outer well. Substituting the asymptotic value of Z, which is equal to the degree of ionization J, into (2.1)–(2.2), and equating $d\Phi(nl|r)/dr$ to zero, we find

$$r_{\text{II min}} = \frac{l(l+1)}{J}, \qquad \Phi(nl|r_{\text{II min}}) = -\frac{J^2}{2l(l+1)}. \tag{3.1}$$

In the neutral atom ($J = 1$) the minimum of the outer well thus lies at 12 a.u. for the f electron, while the wave functions of the core electrons reach out essentially to only 5–6 a.u.; in other words, the outer well has a

TABLE I. Atomic numbers of the elements for which the excited d, f, and g electrons collapse if the core has a normal configuration.[30,44]

Method	Thomas–Fermi	Hartree	Hartree–Fock	Dirac–Fock	Experimental[45]
nl:					
3d	27	21	20		20
4d	45	38	38		38
5d	71	56	56		56
4f	69	58	57		57
6d	>92	88	88	88	88?
5f	>92	90	89	90	
7d			120	120	
6f			120	122	
5g			121	124	

clearly defined hydrogen-like nature. During the collapse of the 4f electron, the average distance from this electron to the nucleus decreases by a factor of about 15, while the binding energy increases by nearly an order of magnitude (Fig. 5). As Z is increased further, the 4f shell is compressed only slightly more rapidly than the outer 5s, 5p, and 6s shells, and the binding energy of the 4f electron remains lower than that of the 5s electron all the way to the middle of the sixth row of the periodic table.[30]

Even more pronounced changes occur during the collapse of a 5g electron. The average radius of its orbit is about 25 a.u. for $Z = 120$, while for $Z = 121$ it is only 0.8 a.u. (Ref. 44). There is also a collapse of 7d and 6f electrons for adjacent elements, so that the elements with $Z = 120$–125 apparently have rather complicated electronic configurations, containing competing 8p, 7d, 6f, and 5g electrons.[44]

For the d electron the minimum of the outer well is at only 6 a.u., and the collapse of this electron leads to much smaller changes in the average distance and binding energy of the electron (Fig. 8). In the following elements the binding energy of the nd electron becomes smaller than that of the $(n+1)s$ electron. In the case of the d electron the shape of the barrier and the particular features of the collapse are highly sensitive to the shell structure of the atom.[30]

For $l = 1$ the centrifugal term is not sufficient for the formation of a potential barrier in the case of neutral atoms or positive ions.[22,30] On the basis of the dependence of the effective charge on the degree of ionization (Fig. 3), however, it may be suggested that a small positive potential barrier may arise even for a p electron in negative ions, and this event would be manifested in certain properties of the negative ions.

The excitation of an electron corresponds to an increase in the effective nuclear charge, so that in a configuration with an inner vacancy electron collapse occurs at a value of Z smaller than for collapse in a configuration with a normal core.[28,46,47]

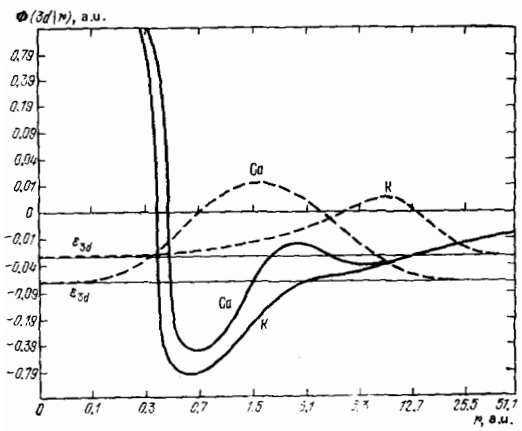

FIG. 8. Collapse of the wave function of a 3d electron between KI3d and CaI4s3d (Ref. 3). Solid curves—effective potential (Hartree–Slater potential); dashed curves—radial wave function (the radial wave functions are drawn as in Fig. 5).

b) Configurations of the type $nl^{4l+1}n'l+1$. The Hartree–Fock average energy approximation

We will discuss in more detail the collapse of d and f electrons in excited configurations of the type $nl^{4l+1}l+1$, which are important in the interpretation of photoabsorption spectra. Furthermore, the collapse has several interesting features in this case.

In an isoelectronic series electron collapse occurs at a lighter element than in the series of neutral atoms. For the $3p^5$ 3d configuration the d electron collapses in the potassium atom rather than in the calcium atom (Table I).[3] The potential barrier for the d electron in the ion is low, so that the contraction of the wave function occurs gradually, over several elements, as is illustrated by the change in the average distance from the 3d electron to the nucleus, $\bar{r}_{3d}$, in Fig. 9.

During the collapse of the 3d electron there is a substantial increase in the overlap of the radial wave function $P(3d|r)$ with the wave function of the 3p electron. This effect increases the electrostatic interaction between these shells: The basic integrals of the direct interaction $[F_2(3p,3d)]$ and of the exchange interaction $[G_1(3p,3d)]$ increase by two orders of magnitude (Fig. 10). There are similar changes in the same integrals when determined by a semiempirical method.[3] During the collapse of a 3d electron there is also a significant increase in the spin–orbit interaction constant $\eta(3d)$, but at low degrees of ionization this constant remains much smaller than $\eta(3p)$, which does not undergo an abrupt change. The collapse of the 3d electron in the isoelectronic series $3p^5$ 3d thus increases the importance of the electrostatic interaction in comparison with the spin–orbit interaction.

In this series there is also an anomalous change in the integral of the dipole transition $(3p|r|3d)$, whose magnitude also depends very strongly on the overlap of the 3p and 3d wave functions (Fig. 11). As we go from ArI to KII the integral approximately doubles in magnitude and begins to decrease monotonically, in the manner typical of an isoelectronic series. On the other hand, the integrals of the transitions of the 3p shell to the 4d and 5d shells show almost no effect of the electron collapse; varying monotonically, they pass through zero, giving rise to the Cooper minimum in the photo-

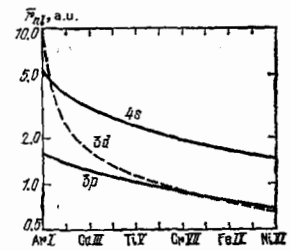

FIG. 9. Change in the average distance from the 3p and 3d electrons to the nucleus in the argon isoelectronic series $3p^5 3d$ and change in the average distance from the 4s electron to the nucleus in the series $3p^5 4s^3$. These results were found from the solutions of the Hartree–Fock equations with the Hartree–Slater potential.

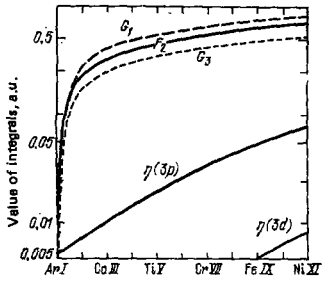

FIG. 10. Changes in the electrostatic-interaction integrals and in the spin–orbit interactions constants in the isoelectronic series ArI3p^{5}3d during collapse of the 3d electron.[3] These results were found from the solutions of the Hartree–Fock equations with the Hartree–Slater potential.

absorption spectrum.[26]

The collapse of a 4f electron in the isoelectronic series XeI4d^{9}4f with the solutions of the Hartree–Fock equations for the average energy was studied in Ref. 27. In this case the one-electron and many-electron values show even larger jumps.

c) Configurations of the type $nl^{4l+1}n'l+1$. Dependence of the electron localization on the particular term

The results described above for the $np^5n'd$ configurations were derived from a potential which ignores those (algebraic) terms which depend on the (energy) term. The incorporation of this dependence in the potential and in the radial wave functions for configurations of this type leads to important refinements, especially for the ^{1}P term.[6,34,48,49]

The ^{1}P term is a special one in the $nl^{4l+1}n'l+1$ configurations in two respects. First, in the expression for the energy of this term the coefficient of the main exchange integral $G_1(nl,n'l+1)$ takes on a large positive value. Accordingly, if the electrostatic interaction between the unfilled shells is stronger than the spin–orbit interaction, the ^{1}P level is a high-lying energy level of this configuration, positioned far from the main group of levels. Second, in the case of LS coupling a dipole transition from a filled shell can go only to the $^1P_1$ level (with an intermediate coupling, there could also be transitions to the $^3P_1$ and $^3D_1$ levels, because of their mixing with $^1P_1$).

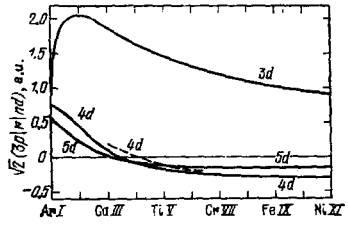

FIG. 11. Change in the integral of the dipole transition $3p^6 \to 3p^5nd$ ($n = 3$–5) in the isoelectronic series ArI$2p^5nd^3$. Solid curves—Calculated with the Hartree–Slater potential; dashed curve—solutions of the Hartree–Fock equations for the average energy. The curves are labelled with the final state, nd.

Since the exchange interaction between unfilled shells is positive, so that the entire exchange term is positive in a certain range of distances from the nucleus, we would be led to believe that this interaction could not be approximated by a statistical potential. The solutions of the Hartree–Fock equations for each term have been used in studying the term dependence of the wave functions of these configurations.

The large exchange (algebraic) term for the ^{1}P (energy) term leads to an important increase in, or to the appearance of, a positive potential barrier at 0.7–1 a.u., i.e., in a region where this energy term makes its maximum contribution to the effective potential.[8,36] For Ar3p^{5}3d, for example, $\Phi(3d^1P|r)$ has a high barrier, with a height reaching 0.7 a.u., and only a small inner well (Fig. 12a), while for the ^{3}P term, as for other terms of the main group, there is only a low negative barrier, and the inner well has a minimum in the region of the positive barrier for ^{1}P. Consequently, the radial wave functions of the 3d electron for these many-electron states are quite different, although both wave functions correspond to an uncollapsed electron.

As we go from ArI to KI the maximum of the radial wave function P(3d LS|r) shifts into the inner well for all the terms except ^{1}P (the barrier essentially disappears; Fig. 12b). The value of $\bar{r}_{3d}(^1P)$ decreases by 1.7 a.u., but the wave function does not collapse. The nature of the one-electron radial wave function here is determined by the many-electron quantum numbers: The radial wave function is localized in different potential wells for different terms of the same atom. As a result, the binding energy of the 3d electron, the electrostatic-interaction integrals, the dipole-transition integral, the constant η(3d), and other quantities show an anomalously strong dependence on the term[34] (for the ^{1}P and ^{3}P terms, the differences in these

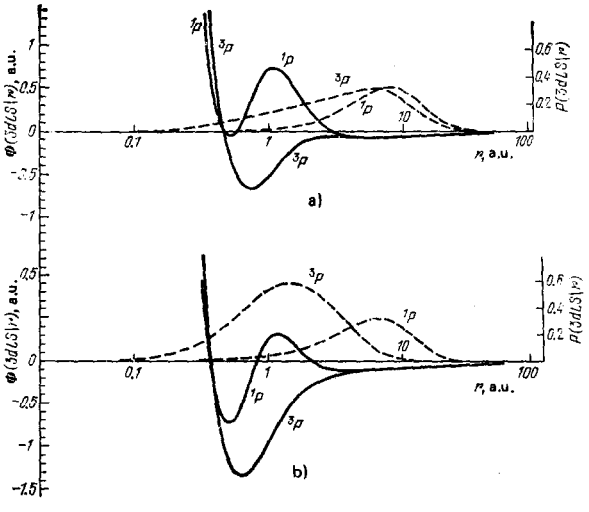

FIG. 12. Term dependence of the collapse of the 3d electron. Dashed curves—The radial wave function P(3d LS|r); solid curves—the effective potential Φ(3d LS|r) for various terms. a) ArI3p^{5}3dLS; b) KI3p^{5}3dLS4s. An average is taken over the electrostatic interaction with the 4s electron in the Hartree–Fock equations for each term for KI (these results were obtained by S. I. Kuchas).

properties are of roughly the same magnitude as the average values for ArI and KII; Figs. 9–11).

The 3d electron in the ^{1}P state does not collapse even for CaI, although its average distance from the nucleus decreases to 6.4 a.u. (Fig. 13a).

Even more gradual is the contraction of the wave function of the 5d electron in the $5p^5$ 5d configuration (Fig. 13b), because there is no positive potential barrier (there is a low negative barrier only for the ^{1}P term[30]).

There is a strong dependence on the many-electron quantum numbers in the case of the clearly defined collapse of a 4f electron for the $4d^9$ 4p configuration, especially for neutral atoms.[6,8]

In the case of XeI the difference between the effective potential in the barrier region for ^{1}P and the other terms [the exchange interaction causes a high hump to appear in $\Phi(4f^1P|r)$ at the barrier; this hump reaches a height of 1.8 a.u.] does not lead to important differences between the uncollapsed radial wave functions; they are hydrogen-like for all terms.[8]

Collapse of the 4f electron in the Hartree–Fock average energy approximation occurs at Ba. When the solutions of the Hartree–Fock equations for each term are used, the wave function for the 4f electron for the lower term of ^{3}P collapses no later than Cs (Fig. 14), while its localization in the ^{1}P state remains nearly the same. The average distances from the 4f electron to the nucleus in the two states differ by a factor of 17 (Table II).

The comparatively large value of $\bar{r}_{4f}$, even for the cesium ion, shows that the 4f electron is still localized in the outer potential well for most of the CsI terms.

In the state corresponding to the ^{1}P term the 4f electron remains far from the nucleus for the following elements (Ba and La), also. On the other hand, the 4f electron in the states of the lower group of terms has

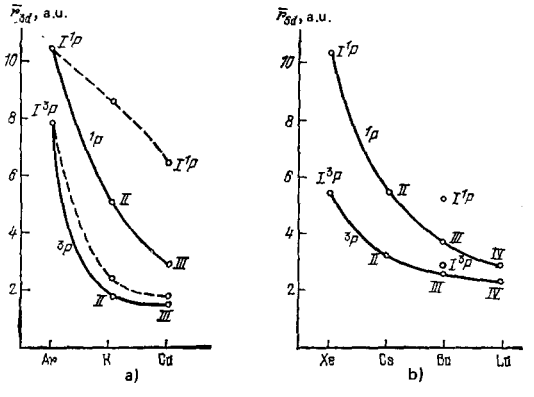

FIG. 13. Dashed curves—Change in the average distance from the 3d and 5d electrons to the nucleus upon the collapse of these electrons in the np^5nd configuration in the series of neutral atoms; solid curves—the same, in the isoelectronic series (after Ref. 34). The curves are labelled with the degree of ionization and the terms $np\,nd$. An average is taken over the interaction with the other vacant shells.

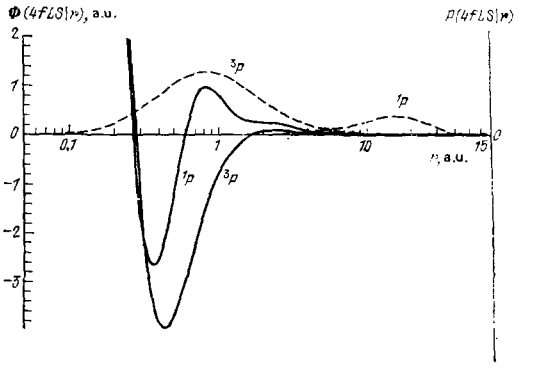

FIG. 14. Localization of the one-electron wave function in various potential wells for various many-electron states of the atom.[8] CsI$4d^94f(LS)6s$ (an average is taken over the interaction with the 6s electron). Solid curves—the effective poteintal $\Phi(4fLS|r)$; dashed curves—radial wave function of the 4f electron. The curves are labelled with the terms.

already collapsed, as is shown by the value of $\bar{r}_{4f}$ obtained in the solutions of the Hartree–Fock equations for the average energy. Interestingly, for barium the function $\Phi(4f^1P|r)$ is complicated, with three wells (Fig. 15). The two barriers are generated by different factors: The barrier closer to the nucleus results from the positive exchange term, while the other results from the centrifugal term. The integrals of the electrostatic interaction between the 4d and 4f shells, the dipole-transition integral, and the spin–orbit interaction constant of the 4f electron increase by two to five orders of magnitude during the collapse of this electron, while in the case of ^{1}P they retain the values characteristic of XeI (Table II). The term dependence of the binding energy of the 4f electron is not as pronounced. In the case of singly charged ions the collapse of the 4f electron in the ^{1}P many-electron state occurs more gradually, from Cs to Ce. The change in $P(4f^1P|r)$ with increasing degree of ionization is shown for barium in Fig. 6.

In summary, the use of the solutions of the Hartree–

TABLE II. Effect of the localization of the 4f electron on various atomic properties as a function of the $4d^94f$ term[8] (in atomic units).

Atom or ion	Term; average energy	$\bar{r}_{4f}$	ε_{4f}	$G_1(4d, 4f)$	$\eta(4f)\cdot10^4$	$(4d\|r\|4f)$
XeI	^{3}D	18.0	−0.031	$6\cdot10^{-6}$	0.001	−0.005
	^{1}P	17.9	−0.031	$1\cdot10^{-5}$	0.001	−0.003
	^{3}P	17.9	−0.031	$1\cdot10^{-5}$	0.001	−0.006
	Av.	18.0	−0.031	$6\cdot10^{-6}$	0.001	−0.005
CsI	^{1}P	17.6	−0.032	$4\cdot10^{-6}$	0.001	−0.004
	^{3}D	17.6	−0.032	$7\cdot10^{-5}$	0.004	−0.013
	^{3}P	1.4	−0.168	0.457	17.9	−0.816
	Av.	17.6	−0.032	$7\cdot10^{-5}$	0.003	−0.12
CsII	^{1}P	8.6	−0.128	$4\cdot10^{-4}$	0.018	−0.042
	^{3}D	2.0	−0.196	0.336	12.4	−0.729
	Av.	6.8	−0.135	0.046	0.159	−0.285
BaI	^{1}P	17.5	−0.032	$2\cdot10^{-5}$	0.002	−0.007
	^{3}P	1.1	−0.559	0.554	26.6	−0.807
	Av.	1.2	−0.382	0.515	24.0	−0.796
BaII	^{1}P	7.5	−0.135	0.003	0.095	−0.086
	^{3}P	1.1	−0.752	0.554	26.6	−0.807
	Av.	1.2	−0.575	0.516	24.1	−0.796
LaI	^{1}P	17.5	−0.032	$3\cdot10^{-5}$	0.002	−0.009
	^{3}P	1.0	−0.885	0.611	35.1	−0.779
	Av.	1.0	−0.692	0.586	33.0	−0.777

Note. For CsI, BaII, and LaI the functional $E(4d^94f(LS)nlL'S')$ and the Hartree–Fock potential for each term are averaged with with respect to the resulting $L'S'$ term.

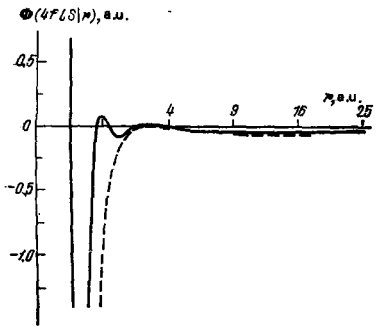

FIG. 15. Effective potential with three wells.[50] Ba|4d^{9}4f. Solid curves—Effective potential for the ^{1}P term; dashed curve—the function $\Phi(4f|r)$ determined with the solutions of the Hartree–Fock equations for the average energy.

Fock equations for the average energy in the case of the configuration $nl^{4l+1}n'l+1$ with a collapsing excited electron can lead to large errors, while the Hartree–Fock approximation for each individual term leads to agreement between the experimental data and the results calculated by more accurate methods, as we will see in the following sections.

d) Abrupt change in the scattering phase shift upon electron collapse

The quantum defect for the Rydberg series, μ_l, depends on the energy of the excited state near the ionization threshold and can be extrapolated beyond the threshold into the continuum.[50-52] Here it is related to the phase shift of the single-channel free-electron wave function, $\delta_l(\varepsilon)$, at $\varepsilon=0$ by

$$\delta_l(0)=\pi\mu_l. \tag{3.2}$$

This relation indicates a strong connection between the positions of the discrete energy levels in the atom and the results on the elastic scattering of electrons by atoms, and it is widely used for a semiempirical determination of the scattering phase shifts.[52]

When the quantum defect of the series changes abruptly upon collapse, the scattering phase shift given by (3.2) should also change abruptly. As the potential barrier rises, the jump in μ_l approaches unity, and the change in $\delta_l(0)$ approaches π. According to Levinson's theorem,[53] $\delta_l(0)$ is equal to the number of bound states multiplied by π [if we assume $\delta_l(\infty)=0$]. The abrupt increase in $\delta_l(0)$ by an amount π thus results from the appearance of a new discrete level in the inner well.

e) Resonant penetration of the wave function of a free electron into the inner part of an atom

An effective potential containing an inner well bounded by a barrier raises the possibility of abrupt change in the wave function of not only a bound electron but also a free electron which is moving in the field of the atom. In such a well, aside from the discrete one-electron levels, there may be levels with a positive energy. When the energy of the free electron is roughly equal to the energy of such a level the electron is captured by the well and forms a quasistationary state or resonance with the atom. The resonances which arise in the single-channel elastic scattering of electrons by atoms are called "shape resonances": They can occur only if the effective potential has a well of spherical shape bounded by a barrier as described above.[9,11]

Shape resonances have been studied in detail in potential-scattering theory[9,53,54]; their existence is attributed to zeros of the Jost function on the complex plane. Here, however, little use has been made of the graphic concept of an effective potential or of the correspondence between the shape of the barrier and the well, on the one hand, and the behavior of the wave function at the resonance energy, on the other, particularly with regard to the penetration of the free-electron wave function into the inner part of the atom. It is the behavior of the wave function in this region which is important in calculating the probabilities for Auger transitions and photoionization cross sections. In a study of their features near the threshold, also resulting from the existence of quasistationary levels in the inner well, the usual approach is to work from the properties of the effective potential.[12,14] These approaches can apparently be mutually complementary, we will accordingly examine the resonance penetration of the wave function of a free electron into the inner part of an atom.

Shape resonances arise during the scattering of an electron by an atom when the orbital angular momentum of the free electron satisfies $l\geq 1$ (Refs. 9 and 53). A potential barrier may also exist in the case of p electron, since the electron scattered by the atom is moving in a field which corresponds to a negative ion in the case of an electron from the discrete spectrum. The outer well is then poorly defined or absent altogether, and the scattering is determined primarily by the inner well and the barrier.

Let us assume that the single-channel wave function $P(\varepsilon l|r)$ is the solution of the Hartree–Fock equations with the following asymptotic condition at infinity:

$$P(\varepsilon l|r)\xrightarrow[r\to\infty]{}k^{-1/2}\sin\left(kr-\frac{l\pi}{2}+\delta_l\right)\quad(k=\sqrt{2\varepsilon}). \tag{3.3}$$

If, instead of the boundary condition at infinity, we require that the radial wave function behave in the limit $r\to 0$ in the same was as the solution for free motion with $V=0$, then we find a regular solution[53] with the asymptotic behavior

$$\overline{P}(\varepsilon l|r)\xrightarrow[r\to\infty]{}|J_0(k)|\,k^{-1/2}\sin\left(kr-\frac{l\pi}{2}+\delta_l\right), \tag{3.4}$$

where $J_0(k)$ is the Jost function.[53]

A resonance corresponds to a zero of the Jost function near the real axis on the complex k plane.[9,53] If the inner well becomes deeper, this zero moves across the $k=0$ axis into the upper half-plane: The resonance disappears, and a bound state appears. This situation corresponds to that in which a level with a positive energy in the inner well moves into the negative energy region as the well becomes deeper.

The probability for finding a particle in the inner part of the atom, divided by the corresponding probability in the absence of interaction forces, is expressed in terms of the reciprocal of the square modulus of the Jost function[54]:

$$\frac{|P(\varepsilon l|r)|^2}{|\overline{P}(\varepsilon l|r)|^2} \xrightarrow[r\to\infty]{} \frac{k^2}{|J_l(k)|^2}. \tag{3.5}$$

In the case of resonance, the point $\bar{k}$, at which $J(\bar{k}) = 0$, lies near the real axis, and near this point the Jost function can be approximated by a series expansion in which only the first term is retained[53]:

$$J_l(\varepsilon) = \left(\frac{dJ_l}{d\varepsilon}\right)_{\bar{\varepsilon}} (\varepsilon - \bar{\varepsilon}) \left(\bar{\varepsilon} = \frac{\bar{k}^2}{2}\right). \tag{3.6}$$

Since k is on the real axis, and $\bar{k} = k_R + ik_I$, we find

$$\frac{|P(\varepsilon l|r)|^2}{|\overline{P}(\varepsilon l|r)|^2} \xrightarrow[r\to 0]{} \left(\frac{dJ_l}{d\varepsilon}\right)_{\bar{\varepsilon}}^{-2} \frac{\varepsilon}{(\varepsilon - \varepsilon_r)^2 + (\Gamma/2)^2}, \tag{3.7}$$

$$\varepsilon_r = \frac{1}{2}(k_R^2 - k_I^2), \quad \Gamma = k_I k_R. \tag{3.8}$$

The lifetime τ of the quasistationary state is related to Γ by $\tau \sim 1/\Gamma$.

Near the resonance, the phase shift, which is equal to minus the argument of the complex quantity $J_l(k)$, is[9]

$$\delta_l(\varepsilon) = \delta_l^0(\varepsilon) - \operatorname{arctg}\frac{\Gamma/2}{\varepsilon - \varepsilon_r}, \tag{3.9}$$

where $\delta_l^0(\varepsilon)$ is the background phase shift, a weak function of the energy. If this background shift is zero, $\delta_l(\varepsilon)$ changes by π when ε passes through the value ε_r. Here the wave function $P(\varepsilon l|r)$, according to (3.7), abruptly penetrates into the inner part of the atom: The node of this function crosses the barrier into the inner well.[14] The penetration of the barrier of $P(\varepsilon l|r)$ occurs more sharply, the larger the orbital angular momentum of the electron, since the imaginary part of the Jost function varies as k^{2l+1} at small k. In other words, as the potential barrier increases (with increasing l) the lifetime τ of the resonance state increases, the resonance width Γ correspondingly decreases, and $P(\varepsilon l|r)$ penetrates the barrier more rapidly.

As ε moves away from ε_r, the probability density of the wave function in the inner part of the atom, according to (3.7), should again decrease, but the nonresonance penetration of $P(\varepsilon l|r)$ into the inner well increases because of the rapid increase in the penetrability of the barrier. There is thus some analogy between the collapse of the free-electron wave function upon the appearance of a discrete spectrum in the inner well and the penetration of the free-electron wave function into the inner well, when the energy of this electron approaches that of a quasistationary level.

These conclusions generally remain valid for a free electron moving in the field of an ion (this statement includes the cases of photoelectrons and Auger electrons).

The resonance penetration of the radial wave function into the atom can be illustrated by the results calculated for $P(\varepsilon l|r)$ for krypton (Fig. 16). At $\varepsilon = 0$, because of the potential barrier, $P(\varepsilon f|r)$ penetrates only slightly into the inner well, and its overlap with the radial wave function of the 3p shell (from which the photoelectron is emitted) is only slight. When ε reaches the energy of the resonance state, the amplitude $P(\varepsilon l|r)$ increases sharply in this region.

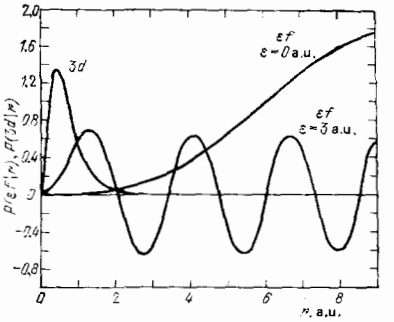

FIG. 16. Penetration of the wave function of a free electron, $P(\varepsilon f|r)$, into the inner part of the atom as the energy ε is increased.[10] Solutions of the self-consistent field equations with the Hartree–Slater potential for krypton. The curves are labelled with the free-electron energy. Also shown here is the radial wave function of the 3d electron.

If ε is approximately equal to ε_r, the function $P(\varepsilon l|r)$ in the inner well becomes similar to the wave function of the discrete level which should form in the inner well as it becomes deeper.[12,31,50] For example, the wave function $P(\varepsilon f|r)$ near the resonance for xenon and the lanthanides is reminiscent of the collapsed wave function[12,55] $P(4f|r)$, while that for uranium and thorium is reminiscent of[56,57] $P(5f|r)$. For a wave function of this type, which describes a "resonantly localized continuum state," the notation $P(\overline{n,\varepsilon f}|r)$ has been suggested.[12,50]

Even when the dependence on the many-electron quantum numbers of the system is taken into account (the solution of the Hartree–Fock equations for each term), the single-channel Hartree–Fock wave function $P(\varepsilon l|r)$ is a comparatively crude approximation for studying the resonances in the elastic scattering of electrons by atoms: Many-electron effects are important in both the continuum and the discrete spectrum of negative ions. More accurate results can be found when $P(\varepsilon l|r)$ is used to calculate the probabilities for Auger transitions [in this application, $P(\varepsilon l|r)$ and even some simpler approximations of this wave function are used in most studies[58]] and also, to a lesser extent, to calculate the cross sections for electron-impact photoionization and ionization of atomic subshells.

4. EFFECT OF ELECTRON COLLAPSE ON THE ARRANGEMENT OF ENERGY LEVELS

a) Anomalous change in the quantum defect as a function of the atomic number and the energy

Study of the collapse of an excited electron has yielded explanations for the abrupt changes in the quantum defect of the spectral series as a function of the atomic number which occur before the beginning of the group of transition elements and the group of rare earths.[45]

As mentioned in the preceding section, the uncollap-

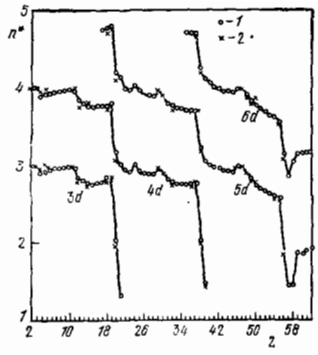

FIG. 17. The effective quantum number n^* of the d electron as a function of the atomic number.[30] 1—Theoretical values (calculated with the Hartree–Slater potential); 2—experimental values, found as the difference between the average energies of the corresponding configurations of the atom and the ion.[45]

sed wave function is hydrogen-like for a two-well potential, and in the transition of the lower level from the outer potential well to the inner well the quantum defect of the series, μ_l, or the effective principal quantum number of the uncollapsed electron of this series,

$$n^* = n - \mu_l = \sqrt{\frac{J_{nl}}{2}} \qquad (4.1)$$

(J_{nl} is the binding energy of the electron), should change by approximately one, taking on integer values.[22,30]

The binding energies calculated with the Hartree–Fock potential, with relativistic effects incorporated in first-order perturbation theory and with the correlation corrections from the statistical model, agree well with experimental data (Figs. 17 and 18). In the case of an f electron, in which the outer well is quite far from the core, the effective quantum number changes by precisely one, while in the case of an excited d electron the jumps are less clearly defined, and n^* depends strongly on the order in which the valence shells are filled.[30,39] The abrupt change in the binding energy corresponds to the atomic numbers listed in Table I.

A similar jump in the quantum defect occurs during electron collapse in an isoelectronic series.[3]

For the Rydberg series of a given element the quantum defect is usually a weak linear function of the excitation energy.[51,52] If the first term of the series is described by a collapsed wave function, while the others are described by uncollapsed hydrogen-like wave functions, the quantum defect for the first term is very different from that for the others.[59,60] In the case of a poorly defined barrier there is a rapid nonlinear change in the defect over the first few terms of the series.[47,61,62]

An anomalous change in the quantum defect and also in the doublet splitting and the spectral density of the oscillator strength, df/dE, has been observed for 5d $\rightarrow nf$ transitions in singley ionized barium[61] (Fig. 19). This change has been explained qualitatively by Hartree–Fock calculations of the radial wave functions

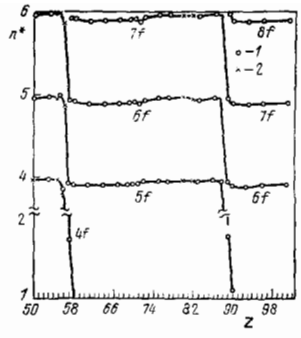

FIG. 18. Effective quantum number n^* of the f electron as a function of the atomic number.[30] The notation is the same as in Fig. 17.

$P(nf|r)$, which have turned out to be distributed in a complicated way between the inner and outer wells[29] (Fig. 7). These calculations confirmed the possibility that the spin–orbit splitting for the 5f electron could be larger than that for the 4f electron, although the value found in the latter case turned out to be too low (Fig. 20). The different overlaps of $P(5d|r)$ with the wave functions $P(nf|r)$ and the cancellation of the positive and negative contributions to the dipole-transition integral $(5d|r|nf)$ can explain the anomalous behavior of the spectral density of the oscillator strength, which has a minimum at $n=5$ and which reaches a maximum at $n=10$–11.

b) The coupling paradox

Electron collapse may be responsible for an anomalous change in the type of coupling within an isoelectronic series. As the degree of ionization increases in an isoelectronic series the coupling ordinarily approaches jj coupling: The spin–orbit interaction increases in proportion to $Z^4(nl)$, while the electrostatic interaction increases only in proportion to $Z(nl)$. As we saw in the example of the p^5d configuration (Fig. 10), however, collapse leads to an opposite effect: an increase in the importance of the electrostatic interaction. This conclusion can be generalized to arbitrary configurations of the type $n_1l_1^{N-1}n_2l_2$ with a collapsing n_2l_2 electron. When the collapse occurs, the electrostatic interaction between the unfilled shells should increase because of an increase in the degree of overlap of the radial wave functions $P(n_1l_1|r)$ and $P(n_2l_2|r)$,

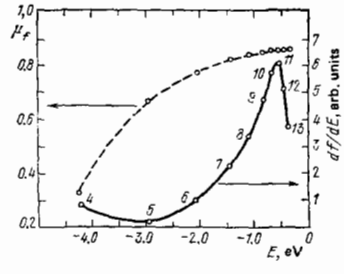

FIG. 19. Dashed curve—Anomalous change in the quantum defect of the nf electron in Ba II; solid curve—spectral density of the oscillator strength df/dE for the transitions $5d \rightarrow nf$ (Ref. 14). Experimental data from Ref. 61. Here E is the level energy reckoned from the ionization limit.

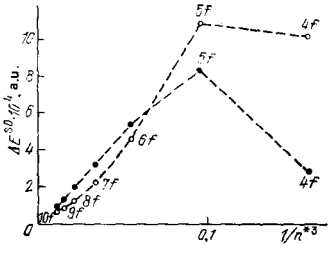

FIG. 20. Spin–orbit splitting of the energy of nf states in Ba II (Ref. 29). Open circles—experimental[61]; filled circles—calculated with the Hartree–Fock potential.

while the spin–orbit interaction, determined primarily by the constant $\eta(n_1l_1)$ for a deeper shell, does not change abruptly during the collapse of the n_2l_2 electron.

Figure 21 illustrates the change in the applicability of the four basic types of coupling (LS, LK, jj, jK) in the isoelectronic series $3p^53d$ and $3p^54d$ with a collapsing nd electron. The square root of the largest weight factor in the expansion of the wave function of the given level in terms of the wave functions for pure types of coupling is adopted as a measure of the purity of the coupling. This quantity is averaged over all the levels of the given configuration. During electron collapse, the LS coupling becomes predominant ($3p^53d$), or merely its applicability improves ($3p^54d$). Further along in the isoelectronic series there is a regular tendency toward jj or jK coupling. A similar tendency is observed when the semiempirical values of the radial integrals are used. These results explain the so-called coupling paradox which has been observed experimentally.[63]

A nonmonotonic change in the type of coupling has also been predicted theoretically for the isoelectronic series $KrI4p^54d$, $XeI5p^55d$, and $SiI5p^54f^3$.

c) Expansion of the energy spectrum and mixing of configurations

In configurations of the type $nl^{4l+1}nl+1$ with a collapsed $nl+1$ electron the width of the energy spectrum is large and may exceed 20 eV, because of a strong electrostatic exchange interaction between unfilled shells, especially in the $^1P_1$ state.[8] Regarding the use of the solutions of the Hartree–Fock equations for the average energy, it has been suggested[64] that the $^1P_1$ level may be pushed out into its own continuum; this suggestion has been used to interpret photoabsorption spectra[65,66] and has been the subject of an extensive debate.[7,12,31,67] The use of the solutions of the Hartree–Fock equations for each term has shown that the wave function of the 4f electron for the ^1P term does not collapse, and this is true not only for Ba but also for La (Table II). In this more accurate approximation the $4d^9$ $4f\ ^1P_1$ level lies below $4d^9\ nf\ ^1P_1$ ($n>4$) and even further below $4d^9\ \varepsilon f\ ^1P_1$ (Refs. 7, 31, and 68). Incorporation of the time dependence in the radial wave functions for the $nl^{4l+1}n'l+1$ configurations makes it possible to eliminate the substantial discrepancies between the experimental and the average-energy Hartree–Fock positions of the $^1P_1$ level.[8,34,49] For such configurations with a collapsing electron, attempts to calculate the spectra by a semiempirical least-squares method with a single set of parameters also fail.

There is also a strong term dependence in configurations of the sp type.[36,37] Although the wave function for the p electron does not collapse, as the wave functions for the d and f electrons in ions do, it is significantly compressed in the elements preceding the beginning of groups with a p shell which is being built up.

During electron collapse there are changes in the energy differences between configurations; a decrease in this difference can lead to a pronounced configuration mixing.[12] During the collapse of the nd electron in CaI($n=3$), SrI($n=4$), and BaI($n=5$) the energy difference between the $nd(n+1)s$ and $(n+1)s^2$ configurations is only 1–3 eV. The $np^5\ nd$ and $np^5\ (n+1)s$ configurations in KII, RbII, and CsII move even closer together.[45] A pronounced mixing of core configura-

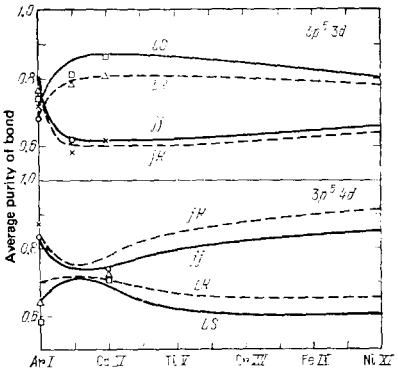

FIG. 21. Effect of the collapse of a d electron on the type of binding in the $3p^53d$ and $3p^54d^3$ configurations. The isoelectronic series of argon. Curves—Results calculated with the Hartree–Slater potential; points—results calculated with semiempirical values of the integrals found by the method of least squares from the experimental energy levels.

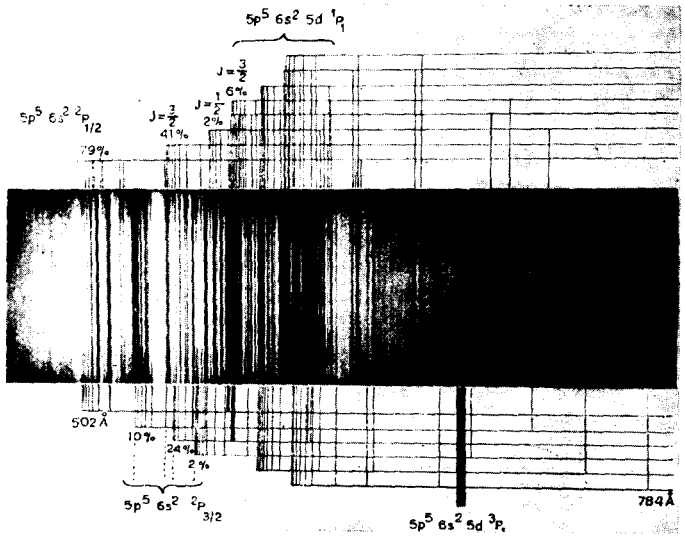

FIG. 22. Spectrum of absorption in the 5p shell of barium vapor.[69] The relative importance of $5p^56s^2\ ^2P$ in the decomposition of the wave functions of the various series was found by a multiconfigurational relativistic calculation.[69]

tions can be responsible for the appearance of additional Rydberg series corresponding to two-electron transitions.[12] In the photoabsorption spectrum from the 5p shell of barium,[69,70] for example, instead of the four series converging to the two limits $5p^5\,^2P_{1/2}$ and $5p^5\,^2P_{3/2}$ there are 14 series, which converge to 12 limits (Fig. 22):

$$5p^6 6s^2 \to 5p^5 (6s^2 + 6s\,5d + 5d^2)\,^2P_{1/2,\,3/2}\,(ns + nd). \qquad (4.2)$$

Calculations by the RPAE method predict one giant absorption resonance in this spectrum.[42] In certain critical cases, therefore, even the partial incorporation of many-electron effects does not guarantee a qualitative agreement with experiment.

5. FEATURES OF ATOMIC ABSORPTION SPECTRA CAUSED BY THE POTENTIAL BARRIER AND ELECTRON COLLAPSE

a) Disappearance of the Rydberg series and shift of the absorption edge

The absorption spectrum corresponding to absorption in an inner shell of a free atom typically has a broad photoionization maximum, abutted on the low-energy side by several Rydberg lines which correspond to transitions to discrete levels. The absorption corresponding to transitions to highly excited levels merges with the photoionization spectrum and forms a sharp absorption edge; the absorption coefficient then falls off monotonically, approaching a hydrogen-like asymptotic behavior at high energies. Absorption in the nl shell can occur by two channels, $\varepsilon l - 1$ and $\varepsilon l + 1$, but the $\varepsilon l + 1$ channel is usually predominant.[20]

If there is a barrier in the effective potential for the $nl + 1$ electron, and all the wave functions $P(nl + 1|r)$ with different values of n are localized in the outer well, far from the atomic core, then the overlap of the wave functions $P(nl|r)$ and $P(n'l + 1|r)$ is slight, and the probability for excitation to the discrete levels $n'l + 1$ is small. As a result, the Rydberg series disappears from the absorption by the nd or nf shells.[12,20] In the case of absorption by an np shell, the overlap of $P(np|r)$ with the uncollapsed wave function $P(n'd|r)$ is not slight, and there may be a "through-the-barrier" excitation, as is observed, for example, in the absorption spectra of 2p and 3p shells of CaI (Refs. 28 and 46).

The existence of a potential barrier also leads to the shift of the absorption edge into the continuum.[20,71] The wave function $P(\varepsilon l + 1|r)$ overlaps slightly with $P(nl|r)$ at small values of ε (Fig. 16), and only when ε approaches the energy of the positive level in the inner well does this wave function suddenly penetrate into the atomic core, leading to the appearance of a resonance in the absorption spectrum. A shift of the absorption edge is observed in the absorption spectra of several elements, by an amount reaching several tens of electron volts. This shift was discovered in the $N_{4,5}$ absorption spectrum of XeI (Refs. 72 and 73), and it was later observed in the absorption spectrum of the 2p shell of Ne and Ar; the 3d shell of Kr, Rb, Sr, and Cd; etc. (see the reviews in Refs. 12 and 20). Two absorption edges, shifted by different amounts, may arise upon absorption in the nf shell; these two edges would correspond to transitions to the channels εd and εg (Refs. 20, 74, and 75).

Figure 23a shows results calculated in the one-electron approximation for the partial cross section $\sigma_{3d\to\varepsilon f}$ for several elements. This cross section exhibits a shifted absorption edge. The cross section $\sigma_{3d\to\varepsilon p}$, on the other hand, reaches its maximum right near the ionization threshold (Fig. 23b). For xenon, $\sigma_{3d\to\varepsilon f}$ and thus σ_{3d} have a sharp resonance according to the one-electron calculations. The experimental spectrum, however, exhibits a rather rounded absorption maximum.[76] A more accurate calculation by the RPAE method with many-electron effects leads to good agreement with experiment.[77] Consequently, when the quasi-stationary one-electron level lies right at the threshold (as is indicated by the sharpness of the resonance) the one-channel calculations can lead to large errors. In general, many-electron effects tend to smooth the resonance peaks in the photoionization spectra.[41,77]

In the spectrum corresponding to absorption by the nl shell ($n > l + 1$), a minimum may appear near the threshold, and there may be a subsequent increase in the ionization cross section, again because the dipole-transition integral crosses zero and changes sign (Fig. 11). This effect may distort the effect of the barrier, so that the effect is seen most clearly in the absorption spectra of the 3d and 4f shells ($n = l + 1$), where the Cooper minimum does not appear.

b) Change in the relative intensities of photoionization and absorption

Upon the collapse of the radial wave function of an $nl + 1$ electron there is a marked increase in the dipole-transition integral (see Fig. 11 and Table II) and thus in the probability for excitation to the first vacant discrete level. As a result, there is a change in the relative intensities of ionization and absorption in the

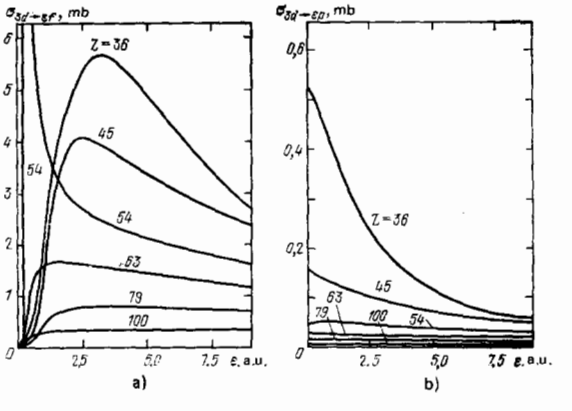

FIG. 23. Photoionization cross sections. a—with a potential barrier; b—without a potential barrier.[10] Results of a one-electron calculation with the Hartree–Slater potential: a) The partial cross section $\sigma_{3d\to\varepsilon f}$ for Kr, Rh, Xe, Eu, Au, and Fm [the maximum of the cross section for $Z = 54$ (Xe) is 13.6 mb at at $\varepsilon = 0.3$ a.u.]; b) the partial cross section $\sigma_{3d\to\varepsilon p}$ for Kr, Rh, Xe, Eu, Au, and Fm.

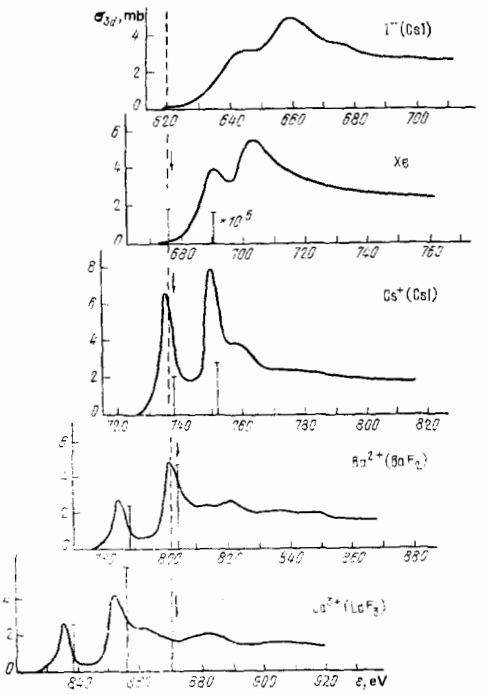

FIG. 24. Change in the $M_{4,5}$ absorption spectrum of xenon-like ions upon the collapse of the 4f electron.[79] The spectra are aligned on the basis of the ionization energies of the $3d_{5/2}$ subshell (the dashed line). Theoretical values of $\sigma_{3d\to 4f}$ (found by the Hartree–Fock method for the average energy) are shown by the vertical lines (for Cs^+, Ba^{2+}, and La^{3+}, these values are reduced by a factor of 1.3; for Xe, they are increased by a factor of 10^5). The arrows show the theoretical ionization edges of the $3d_{5/2}$ subshell.

spectrum, with absorption becoming more intense. This change occurs in the $M_{4,5}$ absorption spectrum for the isoelectronic series of xenon upon the collapse of the 4f electron[78,79] (Fig. 24). (Except for Xe, the species in this series correspond to absorption in ionic compounds, but the similarity of the spectra for the different ionic compounds shows that the spectra are atomic in nature.) In the Xe and I^- spectra there are two broad maxima, which correspond to the M_4 and M_5 absorption edges, as is confirmed by RPAE calculations of the photoionization cross section.[77] The cross section for excitation to an uncollapsed 4f state is negligibly small. Between Xe and Cs^+, the nature of the spectrum changes sharply: The maxima become narrower and shift away from the ionization threshold. Hartree–Fock results show that this change results from the collapse of a 4f electron in the $3d^9$ 4f configuration.[79] The effective nuclear charge is higher for the 4f electron in the $3d^9$ 4f configuration than that in the $4d^9$ 4f configuration, so that the 4f electron collapses as early as Cs^+. The primary maxima in the absorption spectra of Cs^+, Ba^{2+}, and La^{3+} thus correspond to discrete 3d – 4f transitions. This conclusion is confirmed by Hartree–Fock calculations of the photoexcitation cross sections[79] [the agreement with experiment is slightly worse for cesium, demonstrating that cesium is near the critical value Z_c (see Subsec. 2d)]. A similar redistribution of intensity between the excitation and ionization channels has been observed in the $L_{2,3}$ absorption spectrum upon the collapse of a 3d electron in the isoelectronic series of argon, $2p^53d$ (Ref. 80).

c) Nature of the giant absorption resonances

The discrete transitions $nl \to nl+1$ upon the collapse of an $nl+1$ electron may represent the greater part of the oscillator strength: "Giant resonances" or "giant maxima" corresponding to discrete transitions are observed in the absorption spectra. One such resonance is observed in the spectrum of manganese vapor, where it corresponds to the 3p – 3d transition.[81] The large width of the resonance results from intense super-Coster–Kronig transitions.[82] The RPAE calculations describe the shape of the resonance accurately[83] (Fig. 25a). The intense absorption corresponding to transitions to the vacant 3d shell is also characteristic of other elements in the second half of the iron group: Fe, Co, Ni, and Cu (Ref. 85). Giant resonances in the absorption spectra of the vapor of rare earth metals with $Z = 64$–70 near the $O_{2,3}$ threshold have been interpreted as 5p – 5d transitions.[86]

The nature of the broad resonance in the $N_{4,5}$ absorption spectra of lanthanum and barium has been discussed extensively (the spectrum was first obtained for a thin film of metallic lanthanum,[87] but it turned out to be similar to that for the vapor[88]; the absorption spectra of metallic and atomic barium are also quite similar[89]). Calculations for the giant resonances in the $M_{4,5}$ spectra of both elements by the Hartree–Fock method for the average energy have led to the interpretation of these resonances as corresponding to the discrete transitions $4d^{10} - 4d^9 4f\,{}^1P$ (Refs. 64, 66, and 89–91). The solutions of the Hartree–Fock equations for each term for the ^1P term, however, show that the 4f electron in this state is localized in the outer well and that the probability for this transition is very low.[6–8,67] This conclusion agrees with RPAE calculations of the cross section for photoionization from the lanthanum 4d shell,[92] which show that the broad resonance in the $N_{4,5}$ absorption spectrum corresponds to transitions to the continuum.

In the next element, Ce, the 4f electron is now in a normal atomic configuration, and the excitation corresponds to the final configuration $4d^9 4f^2$. For all the terms of this configuration the 4f electron is localized

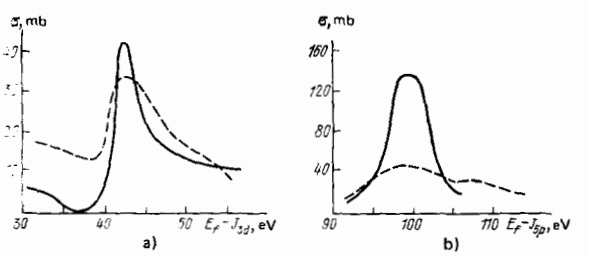

FIG. 25. Giant resonances in the absorption spectra corresponding to discrete transitions.[83] a—$Mn3p^63d^5 \to 3p^53d^6$; b—$Ce4d^{10}4f \to 4d^94f^2$. Dashed curves—experimental[81,83]; solid curves—calculations in the random-phase approximation with exchange. The theoretical maxima along the energy scale are aligned with the experimental maxima; E_f is the photon energy.

in the inner potential well, so that there should be an intensity redistribution between transitions to the discrete and continuous spectra, in agreement with the conclusion that the primary resonance in the $N_{4,5}$ absorption spectrum of cerium is of a discrete nature (this conclusion is reached from calculations of the excitation cross section by the RPAE method; Fig. 25b).

Accordingly, despite the similarity between the $N_{4,5}$ absorption spectrum for La vapor and that for Ce vapor—each spectrum is dominated by a single large resonance—these spectra differ in nature. The intensity redistribution between the discrete and continuous spectra which occurs here is masked by the circumstance that the wave function $P(\varepsilon l|r)$ in the inner well is similar to the wave function $P(4f|r)$, and the discrete level $4d^9 4f\,^1P$ is broad because of a strong interaction with the continuum.

d) Controlled collapse

Connerade has suggested an experiment on "controlled collapse."[5,68] The equilibrium in the case of a collapsed electron is quite sensitive in the sense that the localization of the collapsed electron could be changed gradually by exciting another electron to various states of the Rydberg series. This possibility has been predicted by Hartree–Fock calculations (Fig. 26). If cesium vapor is bombarded simultaneously by a laser beam of a fixed wavelength and by synchrotron radiation, then the localization of the 4f electron in the $4d^9 4f n'l$ configuration will change upon the progressive excitation of the outer nl electron to various $n'l$ states, and this effect will be seen in the spectrum of absorption in the 4d shell.

e) Effect of the barrier on the degree of alignment of ions during photoionization

The existence of an effective potential barrier may be responsible for the increase in the degree of alignment of ions (given a nonuniform occupation of magnetic sublevels) during photoionization of the inner shell of an atom near the ionization threshold.[93]

In the case of an unpolarized primary photon beam the degree of alignment can be characterized by the

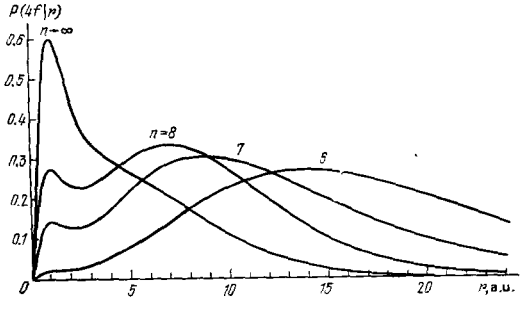

FIG. 26. Change in the wave function of the 4f electron of $CsI4d^9 4fns$ upon the excitation $6s \to ns$. These results illustrate the possibility of a controlled collapse.[5] The calculations were carried out with the Hartree–Fock potential for the average energy. The curves are labelled with the principal quantum number of the excited s electron.

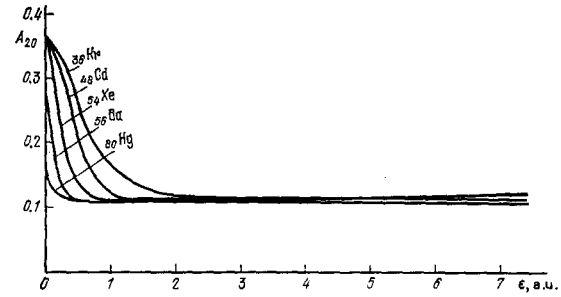

FIG. 27. Degree of alignment of singly charged ions of Kr, Cd, Se, Ba, and Hg with a vacancy in the $3d_{5/2}$ subshell, plotted as a function of the photoelectron energy.[93] The calculations were carried out with the Herman–Skillman potential.

statistical-tensor element A_{20}, which depends on λ, the ratio of the dipole-transition integrals,[93]

$$\lambda = l(l+1)\frac{(nl|r|\varepsilon l-1)}{(nl|r|\varepsilon l+1)}. \qquad (5.1)$$

The element A_{20} reaches a maximum at $\lambda^2 \gg 1$, i.e., when the photoionization channel $l \to l+1$ is weaker than the $l \to l-1$ channel. This situation can arise because of two factors: 1) a suppression of the integral $(nl|r|\varepsilon l+1)$ because of the potential barrier; 2) the appearance of a Cooper minimum upon a change in the sign of this integral. Calculations of the degree of alignment of several shells of various atoms have shown that both effects are important near the photoionization threshold.[93] Figure 27 illustrates the increase in the degree of alignment which results from the existence of a potential barrier during ionization of the $3d_{5/2}$ subshell, in which case there is no Cooper minimum. Alignment of ions can be observed as an anisotropy of the angular distribution of the subsequent emission of x rays or Auger electrons and also as a polarization of the x rays.

6. INTERACTION OF LOW-ENERGY ELECTRONS WITH AN ATOM WITH A TWO-WELL POTENTIAL

a) Shape resonances in the cross section for elastic scattering of electrons

If an electron is moving in an atomic field whose effective potential has a well founded by a barrier, there will be an abrupt change in the scattering phase shift when the electron energy is equal to the energy of the level in the inner well. This jump leads to shape resonances in the partial cross section for elastic scattering of electrons by the atom. The cross section is described by the following expression in the region of the resonance[9,53]:

$$\sigma_r = \sigma_0 \frac{(\varepsilon'+q)^2}{1+\varepsilon'^2}, \qquad (6.1)$$

$$\varepsilon' = \frac{\varepsilon-\varepsilon_r}{\Gamma/2}, \quad q = -\operatorname{ctg}\delta_l^0; \qquad (6.2)$$

ε_r, Γ, and δ_l^0 are defined in (3.8) and (3.9), and σ_0 is the background scattering cross section.

An expression analogous to (6.1) has been derived for the resonance photoionization cross section.[94]

As the orbital angular momentum l of the electron

increases, or (at a given value of l), as the energy of the quasistationary level decreases, the barrier opposing the motion of the electron becomes higher, and the resonance becomes sharper.

A resonance in the partial cross section σ_l can also be seen in the total cross section $\sigma = \sum_l \sigma_l$, since at low energies this cross section is determined primarily by only the first few terms.[53]

Equation (6.1) describes an isolated resonance in the single-channel approximation. When coupling with inelastic-scattering channels is taken into account, other resonances appear, and the phase shift becomes complex.[9,11] Frequently, however, these corrections are small, and the essential behavior of the elastic cross section can be described by a real phase shift.[9]

Shape resonances near the threshold are observed in the elastic scattering of electrons by atoms of alkali metals, alkaline earths, inert gases, etc. (see Refs. 95–97, for example; there are detailed bibliographies in the reviews in Refs. 98 and 99). Although the single-channel wave function calculated with the Hartree–Fock potential and even that calculated with the Hartree potential can be used to study shape resonance in the elastic cross section in certain cases,[100] more accurate methods are ordinarily used for theory of these resonances: the strong-coupling equations, the variational method, etc.[98,99]

b) Existence of a narrow maximum in the bremsstrahlung spectrum

Bombardment of a lanthanum target by electrons of a fixed kinetic energy has revealed a narrow maximum in the bremsstrahlung spectrum near the spectral boundary (Fig. 28). Calculations of the bremsstrahlung spectrum with a Hartree–Slater potential[101] have predicted a structure in the spectrum qualitatively similar to the observed structure, but further from the edge of the spectrum. According to the calculations, the structure derives from a contribution of the f channel of the scattered electron. This partial contribution is characterized by the shift of the maximum away from the edge. An electron which loses almost all its energy by radiation can form a metastable complex with a target atom. The existence of an obstacle—the potential barrier—to the decay of such a complex affects the probability for the emission of a photon of the given energy.[14]

A similar sharp peak near the high-energy boundary of the bremsstrahlung spectrum has also been observed for cerium.[17]

An attempt has been made[17,101,102] to explain the anomalous dependence of the intensity of the $M_{\alpha,\beta}$ x-ray spectrum on the energy of a primary electron beam near the $M_{4,5}$ ionization edges on the basis of a resonance in the bremsstrahlung spectrum. The additional experimental data of Ref. 103 furnish evidence, however, that the resonance x-ray emission here is determined by discrete transitions, rather than by bremsstrahlung, and the variation of the spectrum

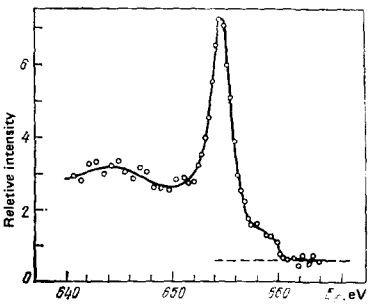

FIG. 28. X-ray bremsstrahlung spectrum emitted upon the scattering of a beam of monoenergetic electrons ($E = 660$ eV) by a lanthanum target.[16]

results from a change in the population of the initial state.

c) Suppression of Auger electron emission during electron-impact ionization of an atom

A phenomenon analogous to a shifted photoionization edge can also occur during electron-impact ionization of atoms. If a shell with a large one-electron orbital angular momentum is ionized, the channels with $l \geq 2$ can be important in the cross section. The scattering along these channels will be affected by the potential barrier, and this effect can lead to a significant suppression of the cross section near the ionization threshold and a subsequent resonant increase of this cross section. The results should be an anomalous dependence of the x-ray and Auger emission on the energy of the electron beam.

Suppression of the Auger electron yield (the integrated intensity over the Auger spectrum) has been observed during ionization of the 4f shell of gold, bismuth, and lead at a beam energy slightly above the binding energy of a 4f electron.[15] The $N_{6,7}O_{4,5}O_{4,5}$ Auger spectrum appears only at a beam energy 60–70 eV greater than the binding energy (Fig. 29a). The yield of Auger electrons during ionization of the 4p or 4d shells, on the other hand, corresponds to the normal ionization threshold: The spectrum is observed immediately, as soon as the beam energy exceeds the binding energy (Fig. 29b).

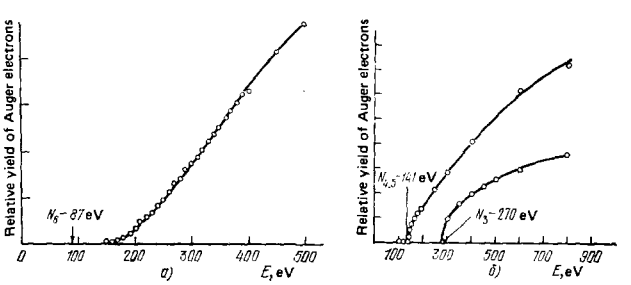

FIG. 29. a—Anomalous; b—normal thresholds for the emission of Auger electrons upon electron-beam ionization of atoms.[15] The arrows show the ionization thresholds; E is the energy of the primary electron beam. a) The auger transitions $N_{6,7}O_{4,5}O_{4,5}$ in gold after ionization of the 4f shell; b) the Auger transitions $N_{4,5}VV$ and $N_3N_{4,5}V$ in gadolinium, which occur after ionization of the 4d and 4p shells, respectively.

A similar suppression of the spectrum near the threshold and a subsequent increase in the intensity upon an increase in the energy of the primary electron beam may also occur in the x-ray emission spectrum. It may be that the threshold observed in the dependence of the cross section for ionization or excitation of the 3d shell on the electron beam energy is related to the change in the intensity in the $M_{\alpha,\beta}$ emission spectra of lanthanum and cerium,[17,101] mentioned in the preceding subsection.

A potential barrier can suppress the emission of low-energy Auger electrons. Although the selection rules permit the emission of Auger electrons with several values of the orbital angular momentum l for most configurations, a single channel is usually dominant in the probability for an Auger transition. If this channel corresponds to $l \geq 2$, the Auger spectrum may be suppressed for certain elements, even though the corresponding Auger transitions are allowed from the energy standpoint. As a result there may be an abrupt increase in the transition probability for another element upon an increase in the transition energy. It is difficult to observe such a phemomenon experimentally because of the difficulties in detecting low-energy Auger electrons.

d) The large post-collision Auger shift

When an Auger spectrum is excited by photons with an energy slightly above the threshold for the formation of the initial vacancy, the energy of the lines in the Auger spectrum is observed to depend on the photon energy. The reason for this effect is the so-called post-collision interaction.[104] The Auger electron is subjected to the Coulomb repulsion of the photoelectron which is moving off slowly and thus the former acquires an increased kinetic energy. The magnitude of this post-collision shift is of the order of 0.1–0.2 eV. Chamberlain *et al.*[17] have observed a large post-collision shift, 1.0 ± 0.2 eV, of the $N_5O_{2,3}O_{2,3}{}^1S_0$ Auger line of Cs^+. The shift of the same line for Xe and I^-, the preceding elements in the isoelectronic series, has a "normal value" (0.04 ± 0.5 and 0.2 ± 0.1 eV). It is for Cs^+ that the 4f electron in the $4d^9 4f\,{}^1P$ many-electron state is at the collapse boundary (see Table I and Fig. 26), so that there is a quasistationary level with a small positive energy in the inner well, and at this photoelectron energy the wave function of the photoelectron should suddenly penetrate into the inner well. As a result, there is a substantial increase in the mutual repulsion of the photoelectron and the Auger electron, which leads to a large post-collision Auger shift. This level in the inner well is much higher for I^- and Xe, and in the energy interval under consideration near the threshold, where the post-collision interaction is manifested, the resonant penetration of the photoelectron wave function into the atom does not occur in these species: The interaction of the photoelectron with the Auger electron is "normal." Chamberlain *et al.*[17] interpret their results as direct proof that a "collapse" of the f wave function of the continuum occurs for Cs^+.

7. CONCLUSION

The existence of a two-well potential and the associated phenomenon of electron collapse may cause anomalous abrupt changes in various atomic spectra: energy spectra, absorption spectra, the spectra of elastic and inelastic electron scattering by atoms, Auger spectra, x-ray emission spectra, etc. The one-electron approximation is usually adequate for explaining these spectral features, although many-electron effects may be important in certain cases for conditions corresponding to a critical equilibrium.

Electron collapse has received little experimental study so far because of the difficulty in carrying out measurements near the thresholds or for highly excited atoms. The theory is also inadequate; there is a particular need for use of the methods of the many-electron theory of the atom.

Clearly defined effects of the potential barrier can be expected in the case of negative ions. The height of the barrier and the conditions of the electron collapse should be affected strongly by external fields.[105]

The effects of the potential barrier in molecules and solids have received even less study than in the case of free atoms. In particular, a distribution of the one-electron wave function between two potential wells might explain why f electrons can participate in chemical bonds, as is indicated by certain results on first- and second-order phase transitions,[106,107] magnetic properties,[106] and the chemical shifts of x-ray lines of rare earth metals and compounds.[108]

Electron collapse is a sensitive indicator of the state of the atom, and this circumstance might be used for high-precision measurements of atomic properties.

I wish to thank S. A. Kuchas and A. V. Karosene for some fruitful discussions and some valuable comments.

[1]E. Fermi, in: Quantentheorie und Chemie (ed. H. Falkenhagen), S. Hinzel-Verlag, Leipzig, 1928, p. 95 (Russ. transl. in Nauchnye trudy, Vol. 1, Nauka, Moscow, 1971, p. 288).
[2]M. Goeppert-Mayer, Phys. Rev. **60**, 184 (1941).
[3]R. D. Cowan, J. Opt. Soc. Am. **58**, 924 (1968).
[4]R. Latter, Phys. Rev. **99**, 510 (1955).
[5]J. P. Connerade, J. Phys. B **11**, L381 (1978).
[6]S. A. Kuchas, A. V. Karosene, and R. I. Karaziya, Opt. Spektrosk. **40**, 764 (1976) [Opt. Spectrosc. **40**, 438 (1976)].
[7]J. E. Hansen, A. W. Fliflet, and H. P. Kelly, J. Phys. B **8**, L175 (1975).
[8]S. A. Kuchas, A. V. Karosene, and R. I. Karaziya, Izv. Akad. Nauk SSSR, Ser. Fiz. **40**, 270 (1976).
[9]P. G. Burke, Potential Scattering in Atomic Physics, Plenum, New York, 1977 (Russ. transl. Atomizdat, Moscow, 1980, Ch. 7).
[10]S. T. Manson and J. W. Cooper, Phys. Rev. **165**, 126 (1968).
[11]V. P. Zhigunov and B. N. Zakhar'ev, Metody sil'noĭ svyazi kanalov v kvantovoĭ teorii rasseyaniya (Methods of Strong Channel Coupling in Quantum Scattering Theory), Atomizdat, Moscow, 1974, p. 81.
[12]J. P. Connerade, Contemp. Phys. **19**, 415 (1978).
[13]T. C. Chiang, D. E. Eastman, F. J. Himpsel, G. Kaindl, and M. Aono, Phys. Rev. Lett. **45**, 1846 (1980).
[14]U. Fano, Phys. Rev. **A12**, 2638 (1975).
[15]D. M. Smith, T. E. Gallon, and J. A. D. Mathew, J. Phys. B

7, 1255 (1974).
[16]R. J. Liefeld, A. G. Burr, and M. B. Chamberlain, Phys. Rev. **A9**, 316 (1974).
[17]M. B. Chamberlain, A. F. Burr, and R. L. Liefield, Phys. Rev. **A9**, 663 (1974).
[18]U. Fano, Comments Atom. and Mol. Phys. **3**, 75 (1972).
[19]J. L. Dehmer, Phys. Fennica **9**, suppl S1, 60 (1974).
[20]U. Fano and J. W. Cooper, Rev. Mod. Phys. **40**, 441 (1968) (Russ. transl. Nauka, Moscow, 1972).
[21]T. Y. Wu, Phys. Rev. **44**, 727 (1933).
[22]A. R. P. Rau and U. Fano, Phys. Rev. **167**, 7 (1968).
[23]R. D. Hartree, The Calculation of Atomic Structures, Wiley, New York, 1957 (Russ. transl., IL, Moscow, 1960).
[24]Ch. Froese-Fischer, The Hartree-Fock Method for Atoms, Wiley, New York, 1977.
[25]F. Herman and S. Skillman, Atomic Structure Calculations Prentice-Hall, Englewood Cliffs, New Jersey, 1963 , pp. 1–8.
[26]J. W. Cooper, Phys. Rev. **128**, 681 (1962).
[27]A. V. Karosene, A. A. Kiselev, and R. I. Karaziya, Litovsk. Fiz. Sb. **13**, 363 (1973).
[28]M. W. D. Mansfield and G. H. Newsom, Proc. R. Soc. **A357**, 77 (1977).
[29]J. P. Connerade and M. W. D. Mansfield, Proc. R. Soc. **A346**, 565 (1975).
[30]D. C. Griffin, K. L. Andrew, and R. D. Cowan, Phys. Rev. **177**, 62 (1969).
[31]G. Wendin, J. Phys. B **9**, L297 (1976).
[32]I. M. Band and V. I. Fomichev, Phys. Lett. **A75**, 178 (1980).
[33]I. M. Band, V. I. Fomichev, and M. B. Trzhaskovskaya, Preprint No. 574, Leningrad Institute of Nuclear Physics, Leningrad, 1980.
[34]S. A. Kuchas and A. V. Karosene, Litovsk. Fiz. Sb. **18**, 187 (1978).
[35]A. A. Kiselev, A. V. Karosene, and R. I. Karaziya, Litovsk. Fiz. Sb. **13**, 375 (1973).
[36]S. A. Kuchas and A. V. Karosene, Litovsk. Fiz. Sb. **20**, 15 (1980).
[37]J. P. Connerade, M. A. Baig, M. W. D. Mansfield, and E. Radtke, Proc. R. Soc. **A361**, 379 (1978).
[38]K. T. Cheng and Y. K. Kim, Opt. Soc. Am. **69**, 125 (1979).
[39]D. C. Griffin, R. D. Cowan, and K. L. Andrew, Phys. Rev. **A3**, 1233 (1971).
[40]A. P. Yutsis, Zh. Eksp. Teor. Fiz. **23**, 357, 371 (1972) [*sic*].
[41]M. Ya. Amusia and N. A. Cherepkov, Case Studies Atomic Phys. **5**, 47 (1975).
[42]G. Wendin, in: Vacuum UV Radiation Physics: Proc. of the Fourth Intern. Conference on VUV Physics, Hamburg, 1974 (ed. E. E. Koch, R. Haensel, and Ch. Kunz-Vieweg), Pergamon, p. 225.
[43]M. Ya. Amus'ya, N. A. Cherepkov, and L. V. Chernysheva, Zh. Eksp. Teor. Fiz. **60**, 160 (1971) [Sov. Phys. JETP **33**, 90 (1971)].
[44]R. D. Cowan and J. B. Mann, in: Atomic Physics Vol. 2: Proc. of the Eleventh Intern. Conference on Atomic Physics, Plenum, New York, 1971, p. 215.
[45]C. E. Moore, Atomic Energy Levels, Circ. No. 467, Vol. 1–3, National Bureau of Standards, Washington, 1949, 1952, 1958.
[46]M. W. D. Mansfield, Proc. R. Soc. **A348**, 143 (1976).
[47]J. P. Connerade, Proc. R. Soc. **347**, 575 (1976).
[48]J. E. Hansen, J. Phys. B **5**, 1096 (1972).
[49]J. E. Hansen, J. Phys. B **5**, 1083 (1972).
[50]G. Wendin and A. F. Starace, J. Phys. B **11**, 4119 (1978).
[51]M. J. Seaton, Proc. Phys. Soc. **88**, 801 (1966).
[52]A. F. Starace, in: Photoionization and Other Probes of Many-Electron Interactions (ed. F. J. Wuilleumier), Plenum, New York, 1975, p. 395.
[53]J. R. Taylor, Scattering Theory: The Quantum Theory on Nonrelativistic Collisions, Wiley, New York, 1972 (Russ. transl. Mir, Moscow, 1975).
[54]R. G. Newton, Scattering Theory of Waves and Particles, McGraw-Hill, New York, 1966 (Russ. transl., Mir, Moscow, 1969).
[55]M. W. D. Mansfield and J. P. Connerade, Proc. R. Soc. **A352**, 125 (1976).
[56]J. P. Connerade, M. W. D. Mansfield, M. Cukier, and M. Pantelouris, J. Phys. B **13**, L235 (1980).
[57]J. P. Connerade, M. Pantelouris, M. A. Baig, M. A. P. Martin, and M. Cukier, J. Phys. B **13**, L357 (1980).
[58]E. J. McGuire, in: Atomic Inner-Shell Processes, Vol. 1: Ionization and Transition Probabilities, Academic, New York, 1975, p. 293.
[59]H. Kleiman, J. Opt. Soc. Am. **52**, 441 (1962).
[60]A. Fröman, J. Linderberg, and Y. Öhrn, J. Opt. Soc. Am. **54**, 1064 (1964).
[61]R. A. Roig and G. Tondello, J. Opt. Soc. Am. **65**, 829 (1975).
[62]B. Elden and P. Risberg, Arkiv Fys. **10**, 553 (1956).
[63]A. H. Gabriel, B. C. Fawcett, and C. Jordan, Proc. Phys. Soc. **87**, 825 (1965).
[64]J. L. Dehmer, A. F. Starace, U. Fano, J. Sugar, and J. W. Cooper, Phys. Rev. Lett. **26**, 1521 (1971).
[65]A. F. Starace, Phys. Rev. **B5**, 1773 (1972).
[66]J. L. Dehmer and A. F. Starace, Phys. Rev. **B5**, 1792 (1972).
[67]A. W. Fliflet, J. P. Kelly, and J. E. Hansen, J. Phys. B **8**, L268 (1975).
[68]J. P. Connerade, J. Phys. B **11**, L409 (1978).
[69]J. P. Connerade, M. W. D. Mansfield, G. H. Newsom, D. H. Tracy, M. A. Baig, and K. Thimm, Phil Trans. R. Soc. **A290**, 327 (1979).
[70]S. J. Rose, J. P. Grant, and J. P. Connerade, Phil. Trans. R. Soc. **A296**, 527 (1979).
[71]J. W. Cooper, Phys. Rev. Lett, **13**, 762 (1964).
[72]A. P. Lukirskiĭ, T. M. Zimkina, and I. A. Brytov, Izv. Akad. Nauk SSSR, Ser. Fiz. **28**, 772 (1964).
[73]D. L. Ederer, Phys. Rev. Lett. **13**, 760 (1964).
[74]F. Combet-Farnaux, J. Phys. **30**, 521 (1969).
[75]J. P. Connerade, B. Drerup, and M. W. D. Mansfield, Proc. R. Soc. **348**, 325 (1976).
[76]R. D. Deslattes, Phys. Rev. Lett. **20**, 483 (1968).
[77]M. Ya. Amus'ya, V. K. Ivanov, S. A. Sheĭnerman, and S. I. Sheftel' Zh. Eksp. Teor. Fiz. **78**, 910 [Sov. Phys. JETP **51**, 458 (1980)].
[78]M. Elango, A. Maiste, and R. Ruus, Phys. Lett. **A72**, 16 (1979).
[79]A. A. Maĭste, R. E. Ruus, S. A. Kuchas, R. I. Karaziya, and M. A. Elango, Zh. Eksp. Teor. Fiz. **78**, 941 (1980) [Sov. Phys. JETP **51**, 474 (1980)].
[80]A. A. Maĭste, R. E. Ruus, and M. A. Elango, Zh. Eksp. Teor. Fiz. **79**, 1671 (1980) [Sov. Phys. JETP **52**, 844 (1980)].
[81]J. P. Connerade, M. W. D. Mansfield, and M. A. P. Martin, Proc. R. Soc. **A350**, 405 (1976).
[82]L. C. Davis and L. A. Feldkamp, Phys. Rev. **A17**, 2012 (1978).
[83]M. Ya. Amusia, V. K. Dolmatov, V. K. Ivanov, and S. I. Sheftel, in: Sixth Intern. Conference on Atomic Physics, Riga, 1978; Abstracts of Contributed Papers (ed. E. Anderson, E. Kraulinya, and R. Peterkop), Riga, 1978, p. 402.
[84]H. W. Wolff, R. Bruhn, K. Radler, and B. Sonntag, Phys. Lett. **A59**, 67 (1976).
[85]R. Bruhn, B. Sonntag, and H. W. Wolff, J. Phys. B **12**, 203 (1979).
[86]D. H. Tracy, Proc. R. Soc. **A357**, 485 (1977).
[87]V. A. Fomichev, T. M. Zimkina, S. A. Gribovskiĭ, and I. I. Zhukova, Fiz. Tverd. Tela (Leningrad) **9**, 1490 (1967) [Sov. Phys. Solid State **9**, 1163 (1967)].
[88]E. R. Radtke, J. Phys. B **12**, L71 (1979).
[89]P. Rabe, K. Radler, and H. W. Wolff, Cited in Ref. 42, p. 247.
[90]I. I. Glembotskiĭ, A. V. Karosene, A. V. Kiselev, A. Yu. Savukinas, S. D. Shadzhyuvene, and A. P. Yutsis, Litovsk. Fiz. Sb. **12**, 235 (1972).
[91]D. L. Ederer, T. B. Lucatorto, E. B. Saloman, R. P. Madden, and J. Sugar, J. Phys. B **8**, L21 (1975).

[92]M. Ya. Amusia and S. I. Sheftel, Phys. Lett. **55**, 469 (1976).
[93]E. G. Berezhko, N. M. Kabachnik, and V. S. Rostovsky, J. Phys. B **11**, 1749 (1978).
[94]U. Fano, Phys. Rev. **124**, 1866 (1961).
[95]A. L. Sinfailam and R. K. Nesbet, Phys. Rev. **A7**, 1987 (1973).
[96]W. Gehenn, J. Phys. B **10**, 3105 (1977).
[97]H. A. Kurtz and Y. Öhrn, Phys. Rev. **A19**, 43 (1979).
[98]R. K. Nesbet, Adv. Atom. and Mol. Phys. **13**, 315 (1977).
[99]R. K. Nesbet, Variational Methods in Electron-Atom Scattering Theory, Plenum, New York, 1980.
[100]N. F. Mott and H. S. W. Massey, The Theory of Atomic Collisions, Oxford University Press, London, 1965 (Russ. transl. Mir, Moscow, 1969).
[101]C. M. Lee and R. H. Pratt, Phys. Rev. **A12**, 707 (1975).
[102]G. Wendin and K. Nuroh, Phys. Rev. Lett. **39**, 48 (1977).
[103]J. Kanski and P. O. Nilsson, Phys. Rev. Lett. **43**, 1185 (1979).
[104]A. Niehaus, J. Phys. B **10**, 1845 (1977).
[105]U. Fano, Collog. Int. CNRS **273**, 127 (1977).
[106]E. M. Savitskii and V. F. Terekhova, Metallovedenie redkozemel'nykh elementov (Metallurgy of the Rare Earths), Nauka, Moscow, 1975, Ch. 2, p. 28.
[107]V. A. Shaburov, I. M. Band, A. I. Grushko, *et al.*, Zh. Eksp. Teor. Fiz. **65**, 1157 (1973) [Sov. Phys. JETP **28**, 573 (1979)].
[108]A. I. Udris, L. L. Makarov, R. I. Karaziya, Yu. M. Zaitsev, D. V. Grabauskas, Yu. O. Bogdanovich, and Yu. F. Batrakov, Primenenie priblizheniya Khartri-Foka k izucheniyu khimicheskikh sdvigov rentgenvskikh linii (Use of the Hartree–Fock Approximation to Study the Chemical Shifts of x-Ray Lines), Deposited Paper No. 1668–78, All-Union Institute for Scientific and Technological Information.

Translated by Dave Parsons